

Correlators of chiral primaries and 1/8 BPS Wilson loops from perturbation theory

Marisa Bonini, Luca Griguolo and Michelangelo Preti

*Dipartimento di Fisica, Università di Parma and INFN Gruppo Collegato di Parma,
Viale G. P. Usberti 7/A, 43100 Parma*

E-mail: marisa.bonini@fis.unipr.it, luca.griguolo@fis.unipr.it,
michelangelo.preti@fis.unipr.it

ABSTRACT: We study at perturbative level the correlation functions of a general class of 1/8 BPS Wilson loops and chiral primaries in $\mathcal{N} = 4$ Super Yang-Mills theory. The contours and the location of operator insertions share a sphere S^2 embedded into space-time and the system preserves at least two supercharges. We perform explicit two-loop computations, for some particular but still rather general configuration, that confirm the elegant results expected from localization procedure. We find notably full consistency with the multi-matrix model averages, obtained from 2D Yang-Mills theory on the sphere, when interacting diagrams do not cancel and contribute non-trivially to the final answer.

KEYWORDS: Wilson, 't Hooft and Polyakov loops, Supersymmetric gauge theory, Duality in Gauge Field Theories, 1/N Expansion

ARXIV EPRINT: [1405.2895](https://arxiv.org/abs/1405.2895)

Contents

1	Introduction and results	1
2	The localization result and multi-matrix models from 2D Yang-Mills	4
3	Perturbative computations I: latitude Wilson loop with an operator insertion at the north-pole of S^2	6
3.1	Ladder contribution I	7
3.2	Interacting contributions I	7
3.3	Summing up interactions I	11
4	Perturbative computations II: equator Wilson loop with an operator insertion at an arbitrary point of S^2	11
4.1	Ladder contribution II	12
4.2	Interacting contributions II	13
4.3	Summing up interactions II	15
A	The integrals $\mathcal{I}_1(x, y)$ and $\mathcal{I}_2(x, y)$	16
B	The latitude-north pole correlator	18
C	Summing up interactions I: the details	19
D	Some useful integrals	22
E	Summing up interactions II: the details	23

1 Introduction and results

In recent years localization has been proven to be one of the most powerful tool in obtaining non perturbative results in quantum supersymmetric gauge theories [1–4]. The key point is that supersymmetry algebras can be often deformed to accommodate background curvature on compact spaces and the resulting partition functions can be computed via a particular saddle-point procedure, known as the supersymmetric localization technique. Thanks to this procedure, an impressive number of new exact results have been derived for supersymmetric theories in different dimensions, mainly when formulated on spheres or products thereof. The technique is enough flexible to compute also correlation functions of local operators and expectation values of non local observables, such as Wilson loops [3, 4] and 't Hooft loops [5, 6]. Actually the exact expression for circular 1/2 BPS Wilson loops in $\mathcal{N} = 4$ Super Yang-Mills theory was conjectured [7, 8] long before its concrete derivation

through supersymmetric localization. This procedure in turn generalizes to a large class of $\mathcal{N} = 2$ theories, where Wilson loops can be also accurately studied [9–11] through matrix model techniques.

In the case of $\mathcal{N} = 4$, the 1/2-BPS circle can be generalized to Wilson loops of arbitrary shapes with lower degree of supersymmetry [12] (for a complete classification see [13, 14]). A particular family within this construction is composed by arbitrary loops lying on a two-sphere S^2 embedded into the Euclidean spacetime. These operators are generically 1/8-BPS, and their quantum correlators seem to be reproduced exactly by a purely perturbative calculation in bosonic 2D Yang-Mills [12, 15]. The original conjecture was substantially proved¹ using supersymmetric localization [16]. The computation in the two-dimensional theory can be exactly mapped to simple Gaussian multi-matrix models [20], leading to an explicit evaluation of the correlators. The relation to 2D YM has been thoroughly checked [21–24] and extended to the inclusion of ’t Hooft loops [25]. Quite interestingly the localization of this family of Wilson loops has been instrumental in deriving a non perturbative expression for the so-called Bremsstrahlung function [26, 27], a non-BPS quantity governing the radiation emitted by an accelerated quark in the small velocity limit. The final result has also been tested using integrability [28, 29], providing a beautiful relation between calculations performed through localization and integrability.

More generally localization should apply not only to the Wilson and ’t Hooft loops, but to a whole sector of operators that are annihilated by shared supercharges. In particular it should concern a family of chiral primary operators inserted on S^2 [30], leading to exact results for their correlators also in presence of Wilson loops. The correlation function of a local operator and a Wilson loop in this sector was firstly computed in [30], supporting and extending the original conjecture of [31] for the correlator of a 1/2-BPS Wilson loop and a chiral primary (see also [32] for the study of the 1/4 BPS case). The correspondence with the zero-instanton sector of two-dimensional YM was checked at tree level, finding consistency with the localization result. In a further development [33] the investigation of the protected sector was extended to the realm of three-point functions. A careful computation of the correlator of two chiral primaries on S^2 with a Wilson loop of arbitrary shape was performed there using a Gaussian three-matrix model. Large R -charge and strong coupling limits were also explored, in order to make contact with the string picture, and interesting results have been obtained considering one “heavy” and one “light” primary [34, 35]. These calculations should be considered important for recent advances on three-point functions study through AdS/CFT duality and integrability [36].

In this paper we take instead a more conservative point of view and study the same correlation functions, considered in [30], through the conventional diagrammatic expansion. Of course the first aim is to check the highly non-trivial reorganization of the perturbative series encoded into the two-matrix model result: localization automatically performs a number of divergences cancellation among different diagrams and combines finite contributions into nice expressions, written in terms of the geometry of the correlator. These effects

¹The Wilson loop operators localize on a 2D gauge theory similar to the Hitchin/Higgs-Yang Mills system [17–19], that is perturbatively equivalent to the usual two-dimensional Yang-Mills theory.

are by no means obvious, especially when the position of the operator and the shape of the contour are arbitrary. The appearing of a gaussian matrix model suggests that only the combinatorics of perturbation theory should mind when bosonic propagators connecting points on the circuit are constant, as for the 1/2 BPS circle in Feynman gauge [7]. In this case the contributions of the interactions, coming from internal loops and non-trivial vertices, should cancel among themselves.² The first situation that we examine reproduces exactly this pattern: we consider a chiral operator inserted on the north-pole of S^2 and a Wilson loop placed on a latitude. The bosonic propagators are constant and we check explicitly the complete cancellation of the interacting diagrams at two-loops: we use dimensional regularization to tame the divergences appearing in the intermediate steps of the calculation and some Mellin-Barnes technology, adapted to our integration contours, to compute the relevant graphs. The resummation of the perturbative exchanges is then easily performed, leading to the expected result. A more involved situation arises when the operator is inserted in an arbitrary point of one of the two hemispheres. The structure of the operator itself changes and the bosonic propagators suspended on the loop are no more constant, complicating the actual computation: in particular the terms involving three contour integrations cannot be reduced completely to double-integrals, as in the previous case. Moreover to evaluate the interacting diagrams we must resort to numerical integration. These diagrams interplay with the ladder ones to reproduce the matrix model result. Once again this picture holds in Feynman gauge and it remains open the possibility to find a gauge in which all the contributions to the correlators originate from the ladder diagrams only, as localization would suggest. In our computation we will consider chiral primaries of dimension $J = 2$: at two-loop this is not really a limitation, in fact one can extend the perturbative evaluation to the general case with some combinatorial effort.³ Furthermore we will analyze explicitly the diagrams in the large N limit, taking into account just the planar contributions. In this way we will compare the perturbative results with the large N solution of matrix model, obtained from localization. The inclusion of non-planar terms can also be easily considered and we checked that they do not change the cancellation pattern.

It would be possible to extend the present computation to the case of two chiral primaries and one Wilson loop, checking in this way the expression derived in [33]. More generally one could try to develop an analogous supersymmetric system in three-dimensional ABJM theory [37], where a family of 1/6 BPS Wilson loops living on the two-sphere S^2 with the same properties of the 1/8 BPS operators considered here has been recently derived [38] and studied at quantum level [39]. Chiral primaries sharing part of the supersymmetries should be constructed and, at least at perturbative level, the correlation function could be studied. We leave these projects for the future.

The structure of the paper is the following. In section 2 we recall the relevant operators (Wilson loops and chiral primaries) and the matrix models describing their correlation functions. In section 3 we outline the computation of the correlation function between

²This statement is gauge dependent and holds in Feynman gauge.

³The basic combination at two-loop level always involve two-legs diagram, so $J = 2$ is the most general situation at this order.

a chiral primary inserted at the north-pole and a latitude Wilson loop: in particular we organize the diagrams and write down the result for the building blocks that cancel among themselves. In section 4 we consider the case of a chiral primary in an arbitrary position. We show that exchange diagrams do not reproduce the matrix model answer and present the contribution of the interaction, organized in basic building blocks. We have various appendices devoted to technical aspects of the computations presented in the body of the paper.

2 The localization result and multi-matrix models from 2D Yang-Mills

The Wilson loops that we consider in this paper are generically 1/8-BPS operators and have been constructed in [12]. They are supported on arbitrary closed curves on a S^2 embedded into the Euclidean four-dimensional space. The relevant two-sphere is defined in Cartesian coordinates as

$$x_4 = 0, \quad \sum_{i=1}^3 x_i^2 = R^2. \quad (2.1)$$

In the following we will take $R = 1$.⁴ To obtain 1/8-BPS Wilson loops one should engineer a suitable coupling with three of the six scalars Φ^i , $i = 1, 2, 3$, of $\mathcal{N} = 4$ SYM and for any contour \mathcal{C} the explicit form of the operator is given by

$$W_{\mathcal{R}}[\mathcal{C}] = \frac{1}{\dim_{\mathcal{R}}} \text{Tr}_{\mathcal{R}} P \exp i \int_{\mathcal{C}} \left[A_i + i \epsilon_{ijk} \Phi^j x_k \right] dx^i, \quad (2.2)$$

where $\dim_{\mathcal{R}}$ denotes the dimension of the representation \mathcal{R} . Because the four supercharges preserved by the loops do not depend on the circuit, a system of Wilson loops on S^2 is 1/8-BPS. Supersymmetry enhances for special shapes: the well-known 1/2-BPS circular Wilson loop is obtained by taking \mathcal{C} to be an equator of S^2 . Circles of arbitrary radius along latitudes of S^2 are 1/4-BPS and they coincide with the 1/4-BPS Wilson loops of [40].

This is not the end of the story: we can also insert an arbitrary number of local operators on the same S^2 still preserving two supercharges. The local operators doing the job are the following

$$\mathcal{O}_J(x) \sim \text{Tr} \left(x_k \Phi^k(x) + i \Phi^4(x) \right)^J \quad x_k \in S^2, \quad k = 1, 2, 3. \quad (2.3)$$

They are of course ordinary chiral primaries, the orientation in the scalar space being simply correlated with the position of the insertion on S^2 . The two-point function of these operators is position independent, as can be easily shown from the direct definition, and, upon choosing a suitable normalization, it holds

$$\langle \mathcal{O}_J(x) \mathcal{O}_{J'}(x) \rangle = \delta_{JJ'}. \quad (2.4)$$

More generally all the n -point functions $\langle \mathcal{O}_{J_1}(x_1) \mathcal{O}_{J_2}(x_2) \dots \mathcal{O}_{J_n}(x_n) \rangle$ are position independent [41] and tree-level exact. Any collection of these operators on S^2 also preserves four

⁴The dependence from the radius of the two-sphere can be easily reintroduced.

supercharges. In presence of the Wilson loops (2.2), the system becomes invariant under two supercharges [30] and mixed correlation functions of Wilson loops and local operators can depend non-trivially on the coupling constant, as we will discuss in the next sections. The two preserved supercharges can be combined [30] to obtain the fermionic charge used in the localization procedure of [16]. Mixed correlators of Wilson loops and local operators should therefore be exactly computed by the perturbative sector two-dimensional Yang-Mills theory on S^2 [15], according to the proposal of [12].

Two-dimensional Yang-Mills theory can be exactly solved on any Riemann surface, both using lattice [42] and localization [43] techniques and its zero-instanton sector is described by certain Gaussian matrix models [20]. The relevant four-dimensional correlators can be eventually mapped to

$$\begin{aligned} & \langle W_{\mathcal{R}_1}[\mathcal{C}_1] W_{\mathcal{R}_2}[\mathcal{C}_2] \dots \mathcal{O}_{J_1}(x_1) \mathcal{O}_{J_2}(x_2) \dots \rangle \\ &= \frac{1}{\mathcal{Z}} \int [dX][dY] \text{Tr}_{\mathcal{R}_1} e^{X_1} \text{Tr}_{\mathcal{R}_2} e^{X_2} \dots \text{Tr} Y_1^{J_1} \text{Tr} Y_2^{J_2} \dots e^{S[X,Y]}, \end{aligned} \quad (2.5)$$

where the matrix model action $S[X, Y]$ is a quadratic form in X_i, Y_i with coefficients depending on the areas singled out by the Wilson loops and the topology of the system. We remark that localization, and consequently the matrix model description, does not need the large N limit.

Special cases of the multi-matrix model (2.5) have been studied and checked in the past: the case of a single Wilson loop has been tested at two-loop [21, 22] and at strong coupling [12] for a non-trivial wedge configuration. Correlators of two Wilson loops were also considered [23, 24] and explicit computations at order g_{YM}^6 have confirmed the matrix model result. The generic n -point function for local operators has been studied in [30] where also the mixed correlator between a Wilson loop and a local operator has been computed and studied in different regimes. Three-point functions have been instead carefully scrutinized in [33], especially at strong coupling and in relation with string computations. Here we concentrate our attention on the mixed two-point correlators:

$$\langle W_{\mathcal{R}}[\mathcal{C}] \mathcal{O}_J(x_1) \rangle = \frac{1}{\mathcal{Z}} \int [dX][dY] \text{Tr}_{\mathcal{R}} e^X \text{Tr} Y^J e^{-\frac{A^2}{2g_{\text{YM}}} \text{Tr} \left(\frac{A_1}{A_2} Y^2 - \frac{2i}{A_2} XY \right)}. \quad (2.6)$$

Here $A_{1,2}$ are the areas single out by the loop on S^2 with $A = A_1 + A_2$ and the local operator is inserted into A_1 . In this paper we will also consider operators normalized as ordinary chiral primaries with unit two-point function

$$\mathcal{O}_J(x) = \left(\frac{2\pi}{\sqrt{\lambda}} \right)^J \frac{1}{\sqrt{J}} \text{Tr} \left(x_k \Phi^k(x) + i \Phi^4(x) \right)^J. \quad (2.7)$$

Taking the trace of the Wilson loop in the fundamental representation and considering the large N limit, the matrix integral (2.6) can be readily done obtaining

$$\langle W_{\mathcal{R}}[\mathcal{C}] \mathcal{O}_J(x_1) \rangle = \frac{1}{N} \frac{\sqrt{J}}{2^J} \left(\frac{A_2}{A_1} \right)^{\frac{J}{2}} I_J(\sqrt{\lambda'}), \quad (2.8)$$

where $\lambda' = 4\lambda A_1 A_2 / A^2$. We will check this expression at second order in perturbation theory. For loops of arbitrary shape and arbitrary operator insertion this result cannot be recovered simply by resumming the ladder exchanges. On the other hand, to perform a concrete computation, we must limit ourselves to some particular configuration, keeping enough generality to observe non-trivially emerging of the matrix model answer. We will consider two cases: in the first one the operator is inserted at the north pole and the loop is placed at an arbitrary latitude. Propagators are constant and interactions should cancel. We then consider a second configuration, where the operator is inserted at an arbitrary point and the loop is wrapped at the equator: here, as we will see, interactions are expected to contribute non-trivially to the final result. In both cases we consider the large N limit, in which just planar contributions are taken into account. The inclusion of non-planar terms do not change the cancellation pattern and just modify, at subleading order in N , the final result, as expected from the matrix model picture.

3 Perturbative computations I: latitude Wilson loop with an operator insertion at the north-pole of S^2

We begin by considering the correlation function between a Wilson loop lying on a latitude of S^2 and a chiral primary operator inserted at the north pole. In our coordinate system the north pole is $x_N = (0, 0, 1, 0)$ and, as a consequence, the CPO operator assumes a very simple form because just two scalars (Φ^3, Φ^4) appear in its explicit expression. It is useful instead to write the Wilson loop through a generalized connection

$$W[\mathcal{C}] = \frac{1}{N} \text{Tr} \mathcal{P} \exp \oint d\tau \mathcal{A}(x(\tau)), \quad (3.1)$$

where

$$\mathcal{A}(x(\tau)) = (iA_\mu \dot{x}^\mu + \sin^2 \theta \Phi^3 - \sin \theta \cos \theta (\sin \tau \Phi^2 + \cos \tau \Phi^1)). \quad (3.2)$$

Here θ is the latitude angle in standard polar coordinates and for symmetry reasons we will restrict its range to $[0, \pi/2]$: at $\theta = 0$ the contour shrinks to the north pole while at $\theta = \pi/2$ we get the equator of S^2 . The position on the latitude is parametrized by τ , ranging from 0 to 2π , and we will denote, in the case of multiple integrations, $x(\tau_i) = x_i$, $\Phi^I(x_i) = \Phi_i^I$ and $\mathcal{A}(x_i) = \mathcal{A}_i$. In Feynman gauge, the effective propagators entering the actual computation do not depend on the positions along the latitude and are the following

$$\begin{aligned} \langle \mathcal{A}_i^{ab} \mathcal{A}_j^{cd} \rangle &= \frac{\lambda'}{16\pi^2} \frac{\delta^{ad} \delta^{bc}}{N}, \\ \langle \mathcal{A}_i^{ab} \Phi^{Icd}(x_N) \rangle &= \frac{\lambda'}{16\pi^2} \frac{\delta_{I3}}{1 - \cos \theta} \frac{\delta^{ad} \delta^{bc}}{N}, \end{aligned} \quad (3.3)$$

where $\lambda' = 4\lambda A_1 A_2 / A^2 = \lambda \sin^2 \theta$ for this loop.

In the following we will restrict our investigation to the case $J = 2$ and at order λ^2 . This choice will simplify our analysis and at two-loop level does not represent a real limitation: no new class of perturbative diagrams would enter the computation and the general case should be tamed by simple combinatorics.

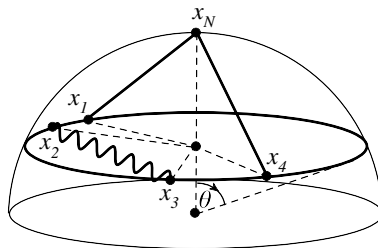


Figure 1. Ladder diagram for latitude-north pole correlation function at order λ^2 .

3.1 Ladder contribution I

Ladder diagrams are the easiest class of perturbative contributions to our correlation function (see figure 1): using the effective propagators (3.3), a straightforward calculation yields

$$\langle W[\mathcal{C}] \mathcal{O}_2(x_N) \rangle_{\text{ladder}} = \frac{1}{N} \frac{\lambda'^2}{192\sqrt{2}} \left(\frac{A_2}{A_1} \right), \quad (3.4)$$

where $\frac{A_2}{A_1} = \cot^2 \frac{\theta}{2}$. Actually it is not difficult to derive the ladder contribution for general J and at any perturbative order (see appendix B): in this case it corresponds to the matrix model result (2.8). Of course (3.4) particularizes this result.

3.2 Interacting contributions I

We discuss now the effect of interaction vertices to the correlation function at order λ^2 : it is the crucial part of the computation. We expect indeed that their total contribution sums to zero since, for the particular configuration we are considering, ladder diagrams are enough to recover the matrix model expression, as shown by (3.4). The different interacting diagrams are grouped in four classes, denoted by **H**, **X**, **IY** and **O**, symbols that actually resemble their graphical form (see figure 2).

The H-contribution. We first consider the diagrams of type **H**: the interaction vertices are connected here by a gluon propagator and its form is

$$-\frac{2}{(2\pi)^2 \lambda} \int_0^{2\pi} d\tau_1 \int_0^{\tau_1} d\tau_2 \int d^4 z d^4 w D(z-w) \langle \text{Tr}(\mathcal{A}_1 \mathcal{A}_2) \text{Tr}(\Phi_z^I \partial_z^\mu \Phi_z^I [\Phi_w^J, \partial_w^\mu \Phi_w^J]) \mathcal{O}_2(x_N) \rangle, \quad (3.5)$$

where $D(x-y) = \frac{1}{(x-y)^2}$. Due to the explicit form of the CPO and of the Wilson loop we have non vanishing contributions from $I = J = 3$. Defining the composite operator $\mathcal{O}_2(x_N)$ via point-splitting

$$(\Phi(x_N))^2 = \lim_{\substack{y_1 \rightarrow x_N \\ y_2 \rightarrow x_N}} \Phi(y_1) \Phi(y_2), \quad (3.6)$$

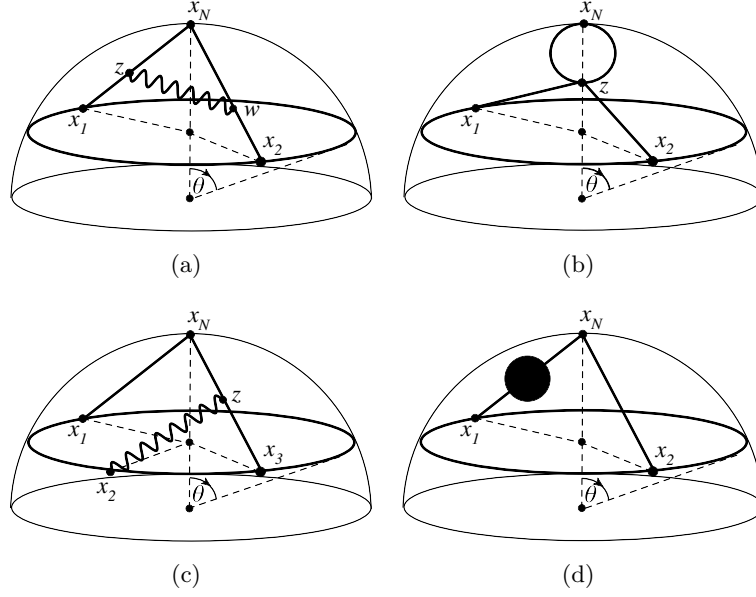


Figure 2. Diagrams with interaction vertices at order λ^2 : (a) **H**-contribution, (b) **X**-contribution, (c) **IY**-contribution and (d) **O**-contribution; z and w denote the position of interaction vertices.

a straightforward manipulation leads to

$$\begin{aligned}
 \mathbf{H} &= \frac{\lambda'^2}{2^2 \sqrt{2} (2\pi)^8 N} \int_0^{2\pi} d\tau_1 \int_0^{\tau_1} d\tau_2 \int d^4 z d^4 w D(z-w) \\
 &\quad \times \left[\left(\partial_{x_1} - \partial_{y_1} \right) \cdot \left(\partial_{x_2} - \partial_{y_2} \right) D(z-y_1) D(w-y_2) D(z-x_1) D(w-x_2) \right. \\
 &\quad \left. + \left(\partial_{x_2} - \partial_{y_1} \right) \cdot \left(\partial_{x_1} - \partial_{y_2} \right) D(w-y_1) D(z-y_2) D(z-x_1) D(w-x_2) \right] \\
 &= \frac{(2\pi)^2 \lambda'^2}{2^2 \sqrt{2} N} \int_0^{2\pi} d\tau_1 \int_0^{2\pi} d\tau_2 (\partial_{x_1} - \partial_{y_1}) \cdot (\partial_{x_2} - \partial_{y_2}) \mathcal{H}(x_1, y_1; x_2, y_2).
 \end{aligned} \tag{3.7}$$

Here we have used the symmetry $z \leftrightarrow w$, symmetrized the expression in the exchange $x_1 \leftrightarrow x_2$ and defined

$$\mathcal{H}(x_1, x_2; x_3, x_4) = \int \frac{d^4 z d^4 w}{(2\pi)^{10}} D(z-x_1) D(z-x_2) D(z-w) D(w-x_3) D(w-x_4). \tag{3.8}$$

Taking advantage of the identity [44]

$$\begin{aligned}
 &(\partial_{x_1} - \partial_{y_1}) \cdot (\partial_{x_2} - \partial_{y_2}) \mathcal{H}(x_1, y_1; x_2, y_2) \\
 &= \frac{1}{(x_1 - y_1)^2 (x_2 - y_2)^2} \left[\mathcal{X}(x_1, y_1, x_2, y_2) \left((x_1 - x_2)^2 (y_1 - y_2)^2 - (x_1 - y_2)^2 (x_2 - y_1)^2 \right) \right. \\
 &\quad \left. + \frac{1}{(2\pi)^2} \left(\mathcal{G}(x_1; x_2, y_2) - \mathcal{G}(y_1; x_2, y_2) + \mathcal{G}(x_2; x_1, y_1) - \mathcal{G}(y_2; x_1, y_1) \right) \right],
 \end{aligned} \tag{3.9}$$

where

$$\begin{aligned}\mathcal{G}(x_1; x_2, x_3) &= \mathcal{Y}(x_1, x_2, x_3)[(x_1 - x_3)^2 - (x_1 - x_2)^2], \\ \mathcal{X}(x_1, x_2, x_3, x_4) &= \frac{1}{(2\pi)^8} \int \frac{d^4 z}{(z - x_1)^2 (z - x_2)^2 (z - x_3)^2 (z - x_4)^2}, \\ \mathcal{Y}(x_1, x_2, x_3) &= \frac{1}{(2\pi)^6} \int \frac{d^4 z}{(z - x_1)^2 (z - x_2)^2 (z - x_3)^2} \equiv \mathcal{I}_1(x_1 - x_3, x_2 - x_3),\end{aligned}\tag{3.10}$$

and setting $y_1 = y_2 = x_N$ we arrive at

$$\begin{aligned}\mathbf{H} &= -\frac{\lambda'^2}{2^2\sqrt{2}N} \oint d\tau_1 d\tau_2 \mathcal{X}(x_1, x_N, x_2, x_N) + \\ &+ \frac{\lambda'^2}{2^2\sqrt{2}N} \frac{1}{1 - \cos\theta} \oint d\tau_1 d\tau_2 \left[\mathcal{I}_1(x_1 - x_N, x_2 - x_N) + \mathcal{I}_1(0, x_2 - x_N) \right] \\ &- \frac{\lambda'^2}{2^3\sqrt{2}N} \frac{1}{(1 - \cos\theta)^2} \oint d\tau_1 d\tau_2 \mathcal{I}_1(x_1 - x_2, x_N - x_2) (x_1 - x_2)^2.\end{aligned}\tag{3.11}$$

The X-contribution. The **X** diagram comes entirely from the four-point scalar vertex

$$\frac{1}{2\lambda} \int_0^{2\pi} d\tau_1 \int_0^{\tau_1} d\tau_2 \int d^4 z \langle \text{Tr}(\mathcal{A}_1 \mathcal{A}_2) \text{Tr}([\Phi_z^I, \Phi_z^J]^2) \mathcal{O}_2(x_N) \rangle.\tag{3.12}$$

The only non vanishing terms arise from $\mathcal{A}_i = \Phi_i^3$ and $I, J = 3, 4$, giving directly

$$\mathbf{X} = \frac{(2\pi)^2 \lambda'^2}{2^2\sqrt{2}N} \int_0^{2\pi} d\tau_1 \int_0^{2\pi} d\tau_2 \mathcal{X}(x_N, x_N, x_1, x_2).\tag{3.13}$$

The IY-contribution. We examine the most elaborate part of the two-loop computation, involving the presence of three distinct contour integrations

$$\frac{i2}{3\lambda} \oint d\tau_1 d\tau_2 d\tau_3 \eta(\tau_1, \tau_2, \tau_3) \int d^4 z \langle \text{Tr}(\mathcal{A}_1 \mathcal{A}_2 \mathcal{A}_3) \text{Tr}(\partial_z^\nu \Phi_z [A_z^\nu, \Phi_z]) \mathcal{O}_2(x_N) \rangle,\tag{3.14}$$

where to take into account the appropriate ordering we have defined

$$\eta(\tau_1, \tau_2, \tau_3) = \theta(\tau_1 - \tau_2)\theta(\tau_2 - \tau_3) + \text{cyclic permutations}.\tag{3.15}$$

Computing the contractions we get

$$\begin{aligned}\mathbf{IY} &= -\frac{\lambda'^2}{2^2\sqrt{2}N} \oint d\tau_1 d\tau_2 d\tau_3 \epsilon(\tau_1, \tau_2, \tau_3) \dot{x}_2^\mu D(x_1 - x_N) \\ &\times \int \frac{d^4 z}{(2\pi)^6} D(x_2 - z) \left[D(x_N - z) \partial_z D(x_3 - z) - \partial_z D(x_N - z) D(x_3 - z) \right],\end{aligned}\tag{3.16}$$

with

$$\epsilon(\tau_1, \tau_2, \tau_3) = \eta(\tau_1, \tau_2, \tau_3) - \eta(\tau_2, \tau_1, \tau_3).\tag{3.17}$$

Performing an integration by parts, we can rewrite \mathbf{IY} as

$$\begin{aligned} \mathbf{IY} &= \frac{\lambda'^2}{2^2\sqrt{2}N} \oint d\tau_1 d\tau_2 d\tau_3 \epsilon(\tau_1, \tau_2, \tau_3) \dot{x}_2^\mu D(x_1 - x_N)(2\partial_3 + \partial_2)\mathcal{Y}(x_2, x_3, x_N) \\ &= \frac{\lambda'^2}{2^2\sqrt{2}N} \frac{1}{1 - \cos\theta} \left\{ \oint d\tau_1 d\tau_3 \left[\mathcal{I}_1(x_1 - x_N, x_3 - x_N) - \mathcal{I}_1(0, x_3 - x_N) \right] \right. \\ &\quad \left. + \oint d\tau_1 d\tau_2 d\tau_3 \epsilon(\tau_1, \tau_2, \tau_3) \dot{x}_2^\mu \partial_3 \mathcal{I}_1(x_3 - x_N, x_2 - x_N) \right\}, \end{aligned} \quad (3.18)$$

where we have used

$$\frac{\partial}{\partial\tau_2} \epsilon(\tau_1, \tau_2, \tau_3) = 2(\delta(\tau_2 - \tau_3) - \delta(\tau_1 - \tau_2)). \quad (3.19)$$

The triple integral can be massaged exploiting the trivial identity

$$\frac{\lambda'^2}{2^2\sqrt{2}N} \frac{1}{1 - \cos\theta} \oint d\tau_1 d\tau_2 d\tau_3 \frac{d}{d\tau_2} \left[\epsilon(\tau_1, \tau_2, \tau_3) \mathcal{I}_2(x_3 - x_N, x_2 - x_N) \right] = 0, \quad (3.20)$$

where the function \mathcal{I}_2 is defined in the appendix A. Upon subtracting (3.20) to (3.18) we obtain

$$\begin{aligned} \mathbf{IY} &= \frac{\lambda'^2}{2^2\sqrt{2}N} \frac{1}{1 - \cos\theta} \left\{ \oint d\tau_1 d\tau_3 \left[\mathcal{I}_1(x_1 - x_N, x_3 - x_N) - \mathcal{I}_1(0, x_3 - x_N) \right] \right. \\ &\quad - 2 \oint d\tau_1 d\tau_3 \left[\mathcal{I}_2(x_3 - x_N, x_3 - x_N) - \mathcal{I}_2(x_3 - x_N, x_1 - x_N) \right] \\ &\quad \left. + \oint d\tau_1 d\tau_2 d\tau_3 \epsilon(\tau_1, \tau_2, \tau_3) \dot{x}_2^\mu V_\mu(x_3 - x_N, x_2 - x_N) \right\}, \end{aligned} \quad (3.21)$$

with

$$V^\mu(x, y) \equiv \partial_x^\mu \mathcal{I}_1(x, y) - \partial_y^\mu \mathcal{I}_2(x, y). \quad (3.22)$$

With the help of equation (A.11) we find

$$\begin{aligned} \dot{x}_2^\mu V_\mu(x_3 - x_N, x_2 - x_N) &= - \frac{1}{32\pi^4(x_3 - x_N)^2} \frac{d}{dt_2} \left[\text{Li}_2 \left(1 - \frac{(x_3 - x_2)^2}{(x_2 - x_N)^2} \right) \right. \\ &\quad \left. + \frac{1}{2} \log^2 \left[\frac{(x_3 - x_2)^2}{(x_2 - x_N)^2} \right] - \frac{1}{2} \log^2 \left[\frac{(x_3 - x_2)^2}{(x_3 - x_N)^2} \right] \right]. \end{aligned} \quad (3.23)$$

Inserting this result into (3.21) and integrating by parts we arrive at the final expression

$$\begin{aligned} \mathbf{IY} &= \frac{\lambda'^2}{2^2\sqrt{2}N} \frac{1}{1 - \cos\theta} \left\{ \oint d\tau_1 d\tau_3 \left[\mathcal{I}_1(x_1 - x_N, x_3 - x_N) - \mathcal{I}_1(0, x_3 - x_N) \right] \right. \\ &\quad - 2 \oint d\tau_1 d\tau_3 \left[\mathcal{I}_2(x_3 - x_N, x_3 - x_N) - \mathcal{I}_2(x_3 - x_N, x_1 - x_N) \right] \\ &\quad \left. - \frac{1}{2^6\pi^4} \frac{1}{1 - \cos\theta} \oint d\tau_1 d\tau_3 \left[\text{Li}_2 \left(1 - \frac{\sin^2\theta}{1 - \cos\theta} (1 - \cos\tau_{31}) \right) - \frac{\pi^2}{6} \right] \right\}, \end{aligned} \quad (3.24)$$

where $\tau_{ij} = \tau_i - \tau_j$.

The O-contribution. The last interacting diagram comes from the self-energy of the scalar propagator: borrowing directly the result from [7], we write down

$$\mathbf{O} = -\frac{\lambda'^2}{2\sqrt{2}N} \frac{1}{1 - \cos \theta} \oint d\tau_1 d\tau_2 \mathcal{I}_1(0, x_2 - x_N). \quad (3.25)$$

3.3 Summing up interactions I

Adding up the contributions of all the interacting diagrams we obtain:

$$\begin{aligned} \langle W[\mathcal{C}] \mathcal{O}_2(x_N) \rangle_{\text{int}} &= \mathbf{H} + \mathbf{O} + \mathbf{X} + \mathbf{IY} = \\ &= -\frac{\lambda'^2}{2^3 \sqrt{2} N} \frac{1}{(1 - \cos \theta)^2} \oint d\tau_1 d\tau_2 \mathcal{I}_1(x_1 - x_2, x_N - x_2) (x_1 - x_2)^2 \\ &+ \frac{\lambda'^2}{2\sqrt{2}N} \frac{1}{1 - \cos \theta} \oint d\tau_1 d\tau_2 \left[\mathcal{I}_1(x_1 - x_N, x_2 - x_N) + \mathcal{I}_2(x_2 - x_N, x_1 - x_N) \right] \\ &- \frac{\lambda'^2}{2\sqrt{2}N} \frac{1}{1 - \cos \theta} \oint d\tau_1 d\tau_2 \left[\mathcal{I}_2(x_2 - x_N, x_2 - x_N) + \mathcal{I}_1(0, x_2 - x_N) \right] \\ &- \frac{\lambda'^2}{2^8 \pi^4 \sqrt{2} N} \frac{1}{(1 - \cos \theta)^2} \oint d\tau_1 d\tau_2 \left[\text{Li}_2 \left(1 - \frac{\sin^2 \theta}{1 - \cos \theta} (1 - \cos \tau_{21}) \right) - \frac{\pi^2}{6} \right]. \end{aligned} \quad (3.26)$$

Remarkably, no triple contour integration is present in this final expression. The integrals in (3.26), denoted by $P_{1,2,3,4}$, are evaluated in appendix C. Using these results we find

$$\langle W[\mathcal{C}] \mathcal{O}_2(x_N) \rangle_{\text{int}} = -\frac{\lambda'^2}{2^3 \sqrt{2} N} \frac{1}{(1 - \cos \theta)^2} \left[P_1 - \frac{1 - \cos \theta}{4} (P_2 - P_3) + \frac{P_4}{2^5 \pi^4} - \frac{1}{3 \cdot 2^4} \right] = 0 \quad (3.27)$$

for any θ , as expected. We confirm therefore that at order λ^2 , the correlator of the latitude Wilson loop with \mathcal{O}_2 at the north-pole is

$$\langle W[\mathcal{C}] \mathcal{O}_2(x_N) \rangle = \langle W[\mathcal{C}] \mathcal{O}_2(x_N) \rangle_{\text{ladder}} = \frac{1}{N} \frac{\lambda'^2}{192\sqrt{2}} \left(\frac{A_2}{A_1} \right). \quad (3.28)$$

4 Perturbative computations II: equator Wilson loop with an operator insertion at an arbitrary point of S^2

In this section we consider the correlation function of a Wilson loop shaped on the equator of S^2 and the CPO operator (2.7) inserted on the sphere at the point $x_{\mathcal{O}} = (\sin \phi, 0, \cos \phi)$ (one of the coordinates can be taken to zero by symmetry reasons). Without loss of generality, we also assume that the operator is located in the north hemisphere, and we consider $0 \leq \phi \leq \pi/2$. Thus the CPO depends on the three scalars Φ^I , with $I = 1, 3, 4$ and the Wilson loop is written as an integral of the generalized connection as in (3.1) with

$$\mathcal{A}(x(\tau)) = (iA_\mu \dot{x}^\mu + \Phi^3). \quad (4.1)$$

In Feynman gauge, the effective propagators are now the following:

$$\begin{aligned}\langle \mathcal{A}_i^{ab} \mathcal{A}_j^{cd} \rangle &= \frac{\lambda}{16\pi^2} \frac{\delta^{ad} \delta^{bc}}{N}, \\ \langle \mathcal{A}_i^{ab} \Phi^{Icd}(x_{\mathcal{O}}) \rangle &= \frac{\lambda}{16\pi^2} f(\tau_i) \cos \phi \frac{\delta^{ad} \delta^{bc}}{N} \delta_{I3},\end{aligned}\quad (4.2)$$

where

$$f(\tau_i) = \frac{1}{1 - \sin \phi \cos \tau_i}. \quad (4.3)$$

Notice that a new and relevant feature appears in this case: effective propagators connecting the CPO and the Wilson loop depend explicitly on the integration parameters τ_i . As we will see soon, this aspect complicates considerably the computations and, crucially, destroys the naive matrix model picture based on summing up ladder diagrams and neglecting interaction vertices. Unfortunately we will not be able to perform all the calculations analytically and we will resort to numerical integration for one particular contribution. We again limit ourselves to CPO with $J = 2$.

4.1 Ladder contribution II

At the order λ^2 , the ladder contribution (see figure 3) arises from

$$\langle W[\mathcal{C}] \mathcal{O}_2(x_{\mathcal{O}}) \rangle_{\text{ladder}} = \frac{1}{N} \int_0^{2\pi} d\tau_1 \int_0^{\tau_1} d\tau_2 \int_0^{\tau_2} d\tau_3 \int_0^{\tau_3} d\tau_4 \langle \text{Tr}(\mathcal{A}_1 \mathcal{A}_2 \mathcal{A}_3 \mathcal{A}_4) \mathcal{O}_2(x_{\mathcal{O}}) \rangle. \quad (4.4)$$

By performing the contractions and using (4.2), we find

$$\frac{\lambda^2 \cos^2 \phi}{29\sqrt{2}\pi^4 N} \int_0^{2\pi} d\tau_1 \dots \int_0^{\tau_3} d\tau_4 \left[f(\tau_1)f(\tau_4) + f(\tau_1)f(\tau_2) + f(\tau_2)f(\tau_3) + f(\tau_3)f(\tau_4) \right]. \quad (4.5)$$

By simply changing the integration order, we can evaluate two integrals, ending up with

$$\begin{aligned}& \frac{\lambda^2 \cos^2 \phi}{29\sqrt{2}\pi^4 N} \int_0^{2\pi} d\tau_1 f(\tau_1) \int_0^{\tau_1} d\tau_2 f(\tau_2) \left[(\tau_1 - \tau_2)^2 + 2\pi^2 - 2\pi(\tau_1 - \tau_2) \right] \\ &= \frac{\lambda^2 \cos^2 \phi}{29\sqrt{2}\pi^4 N} \left[\mathcal{J}_2 \mathcal{J}_0 - \mathcal{J}_1^2 + \pi^2 \mathcal{J}_0^2 - 2\pi \mathcal{J}_1 \mathcal{J}_0 + 4\pi \tilde{\mathcal{J}} \right],\end{aligned}\quad (4.6)$$

where \mathcal{J}_n e $\tilde{\mathcal{J}}$ are defined and computed in appendix D. Using these results we get

$$\begin{aligned}\langle W[\mathcal{C}] \mathcal{O}_2(x_{\mathcal{O}}) \rangle_{\text{ladder}} &= \\ &= \frac{\lambda^2}{192\sqrt{2}N} - \frac{\lambda^2}{26\sqrt{2}\pi^2} \left[\log\left(\frac{2\sigma}{1+\sigma}\right)^2 + \log\left(\frac{1+\sigma}{2}\right)^2 + 2\text{Li}_2\left(\frac{1-\sigma}{2}\right) + 2\text{Li}_2\left(\frac{\sigma-1}{2\sigma}\right) \right],\end{aligned}\quad (4.7)$$

where $\sigma = \sqrt{\frac{1+\sin \phi}{1-\sin \phi}}$.

The first term in the above expression already gives the matrix model result, i.e. the second order term in the expansion of Bessel $I_2(\sqrt{\lambda})$. Therefore the remaining term

$$\mathbf{L} \equiv -\frac{\lambda^2}{26\sqrt{2}\pi^2} \left[\log\left(\frac{2\sigma}{1+\sigma}\right)^2 + \log\left(\frac{1+\sigma}{2}\right)^2 + 2\text{Li}_2\left(\frac{1-\sigma}{2}\right) + 2\text{Li}_2\left(\frac{\sigma-1}{2\sigma}\right) \right] \quad (4.8)$$

should cancel the interacting contributions.

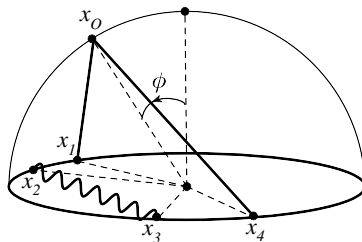


Figure 3. Ladder diagram for equator-arbitrary point correlation function at order λ^2 .

4.2 Interacting contributions II

We attempt here the computation of the diagrams containing interaction vertices (see figure 4): due to the asymmetry of our configuration we will not be able to obtain an expression only in terms of double-integrals, as in the previous case. We have truly to face triple contour integrations, and moreover part of the job must be done numerically.

The H, X and O contributions. The procedure to evaluate the diagrams **H**, **O** e **X** is very similar to the previous case. Their structure remains basically unchanged, the only relevant difference being the appearance of contour dependent propagators. We get

$$\begin{aligned} \mathbf{H} = & -\frac{(2\pi)^2 \lambda^2 \cos^2 \phi}{2^2 \sqrt{2} N} \oint d\tau_1 d\tau_2 \mathcal{X}(x_1, x_O, x_2, x_O) \\ & + \frac{\lambda^2 \cos^2 \phi}{2^2 \sqrt{2} N} \int_0^{2\pi} d\tau_1 f(\tau_1) \int_0^{2\pi} d\tau_2 \left[\mathcal{I}_1(x_1 - x_O, x_2 - x_O) + \mathcal{I}_1(0, x_2 - x_O) \right] \\ & - \frac{\lambda^2 \cos^2 \phi}{2^3 \sqrt{2} N} \int_0^{2\pi} d\tau_1 f(\tau_1) \int_0^{2\pi} d\tau_2 f(\tau_2) \mathcal{I}_1(x_1 - x_2, x_O - x_2) (x_1 - x_2)^2, \end{aligned} \quad (4.9)$$

$$\mathbf{X} = \frac{(2\pi)^2 \lambda^2 \cos^2 \phi}{2^2 \sqrt{2} N} \oint d\tau_1 d\tau_2 \mathcal{X}(x_O, x_O, x_1, x_2), \quad (4.10)$$

$$\mathbf{O} = -\frac{\lambda^2 \cos^2 \phi}{2^3 \sqrt{2} N} \int_0^{2\pi} d\tau_1 f(\tau_1) \int_0^{2\pi} d\tau_2 \mathcal{I}_1(0, x_2 - x_O), \quad (4.11)$$

with the functions \mathcal{X} e \mathcal{I}_1 defined in (3.10).

The IY-contribution. We have seen in the previous section, that the **IY** diagram contains triple integrations along the circuit. In that case we have been able, through some judicious manipulation, to reduce the problem to double integrals. Now, with the CPO operator in an arbitrary position on the sphere, this technique works only partially.

Repeating the same steps as in section 3 we arrive at the expression

$$\begin{aligned} \mathbf{IY} = & \frac{\lambda^2 \cos^2 \phi}{2^2 \sqrt{2} N} \oint d\tau_1 f(\tau_1) \left\{ \oint d\tau_3 \left[\mathcal{I}_1(x_1 - x_O, x_3 - x_O) - \mathcal{I}_1(0, x_3 - x_O) \right] \right. \\ & \left. + \oint d\tau_2 d\tau_3 \epsilon(\tau_1, \tau_2, \tau_3) \dot{x}_2^\mu \partial_3 \mathcal{I}_1(x_3 - x_O, x_2 - x_O) \right\}. \end{aligned} \quad (4.12)$$

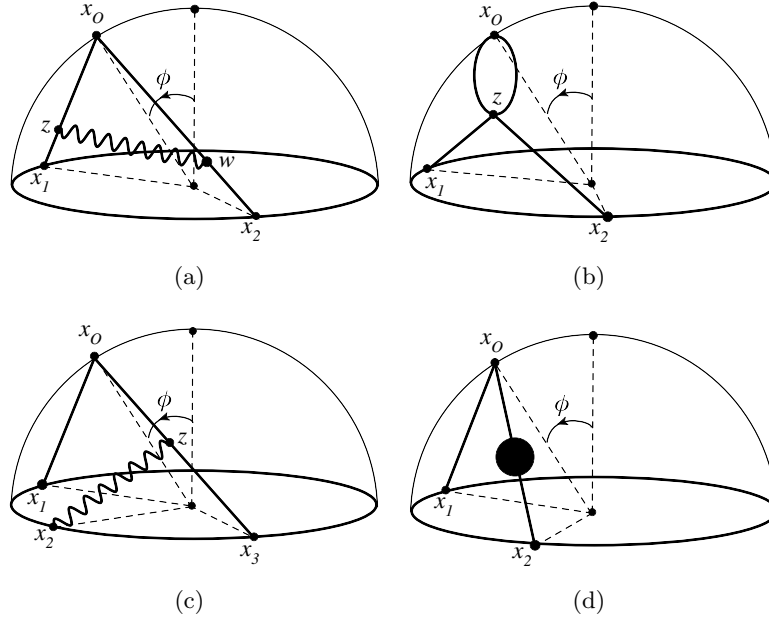


Figure 4. Diagrams with interaction vertices at order λ^2 : (a) **H**-contribution, (b) **X**-contribution, (c) **IY**-contribution and (d) **O**-contribution; z and w denote the position of interaction vertices.

We can still massage the triple integral using an identity similar to (3.20), obtaining

$$\begin{aligned}
 \mathbf{IY} = & \frac{\lambda^2 \cos^2 \phi}{2^2 \sqrt{2} N} \oint d\tau_1 f(\tau_1) \left\{ \oint d\tau_3 \left[\mathcal{I}_1(x_1 - x_{\mathcal{O}}, x_3 - x_{\mathcal{O}}) - \mathcal{I}_1(0, x_3 - x_{\mathcal{O}}) \right] \right. \\
 & - 2 \oint d\tau_3 \left[\mathcal{I}_2(x_3 - x_{\mathcal{O}}, x_3 - x_{\mathcal{O}}) - \mathcal{I}_2(x_3 - x_{\mathcal{O}}, x_1 - x_{\mathcal{O}}) \right] \\
 & \left. + \oint d\tau_2 d\tau_3 \epsilon(\tau_1, \tau_2, \tau_3) \dot{x}_2^\mu V_\mu(x_3 - x_{\mathcal{O}}, x_2 - x_{\mathcal{O}}) \right\}.
 \end{aligned} \tag{4.13}$$

Using again (A.11), we end up with

$$\begin{aligned}
 \mathbf{IY} = & \frac{\lambda^2 \cos^2 \phi}{2^2 \sqrt{2} N} \oint d\tau_1 f(\tau_1) \left\{ \oint d\tau_3 \left[\mathcal{I}_1(x_1 - x_{\mathcal{O}}, x_3 - x_{\mathcal{O}}) - \mathcal{I}_1(0, x_3 - x_{\mathcal{O}}) \right] \right. \\
 & - 2 \oint d\tau_3 \left[\mathcal{I}_2(x_3 - x_{\mathcal{O}}, x_3 - x_{\mathcal{O}}) - \mathcal{I}_2(x_3 - x_{\mathcal{O}}, x_1 - x_{\mathcal{O}}) \right] \\
 & - \frac{1}{2^6 \pi^4} \oint d\tau_3 f(\tau_3) \left[\text{Li}_2 \left(1 - (1 - \cos \tau_{31}) f(\tau_1) \right) - \frac{\pi^2}{6} \right] \\
 & \left. + \frac{1}{2^7 \pi^4} \oint d\tau_2 d\tau_3 \epsilon(\tau_1, \tau_2, \tau_3) f(\tau_3) \cot \left(\frac{\tau_{32}}{2} \right) \log \left(\frac{f(\tau_3)}{f(\tau_2)} \right) \right\}.
 \end{aligned} \tag{4.14}$$

Unfortunately, in this case the awkward triple integral cannot be avoided.

4.3 Summing up interactions II

The evaluation of the whole interacting contributions requires some care: first of all let us collect the different diagrams

$$\begin{aligned}
 \langle W[\mathcal{C}] \mathcal{O}_2(x_{\mathcal{O}}) \rangle_{\text{int}} &= \mathbf{H} + \mathbf{O} + \mathbf{X} + \mathbf{IY} = \\
 &- \frac{\lambda^2 \cos^2 \phi}{2^3 \sqrt{2} N} \oint d\tau_1 d\tau_2 f(\tau_1) f(\tau_2) \mathcal{I}_1(x_1 - x_2, x_{\mathcal{O}} - x_2) (x_1 - x_2)^2 \\
 &+ \frac{\lambda^2 \cos^2 \phi}{2 \sqrt{2} N} \oint d\tau_1 d\tau_2 f(\tau_1) \left[\mathcal{I}_1(x_1 - x_{\mathcal{O}}, x_2 - x_{\mathcal{O}}) + \mathcal{I}_2(x_2 - x_{\mathcal{O}}, x_1 - x_{\mathcal{O}}) \right] \\
 &- \frac{\lambda^2 \cos^2 \phi}{2^8 \pi^4 \sqrt{2} N} \oint d\tau_1 d\tau_2 f(\tau_1) f(\tau_2) \left[\text{Li}_2 \left(1 - (1 - \cos \tau_{21}) f(\tau_1) \right) - \frac{\pi^2}{6} \right] \\
 &- \frac{\lambda^2 \cos^2 \phi}{2 \sqrt{2} N} \oint d\tau_1 d\tau_2 f(\tau_1) \left[\mathcal{I}_2(x_2 - x_{\mathcal{O}}, x_2 - x_{\mathcal{O}}) + \mathcal{I}_1(0, x_2 - x_{\mathcal{O}}) \right] \\
 &+ \frac{\lambda^2 \cos^2 \phi}{2^9 \pi^4 \sqrt{2} N} \oint d\tau_1 d\tau_2 d\tau_3 \epsilon(\tau_1, \tau_2, \tau_3) f(\tau_1) f(\tau_3) \cot \left(\frac{\tau_{32}}{2} \right) \log \left(\frac{f(\tau_3)}{f(\tau_2)} \right). \tag{4.15}
 \end{aligned}$$

Using the definitions in appendix A we can simplify this expression noticing that

$$\begin{aligned}
 \left[\mathcal{I}_2(x_2 - x_{\mathcal{O}}, x_2 - x_{\mathcal{O}}) + \mathcal{I}_1(0, x_2 - x_{\mathcal{O}}) \right] &= - \lim_{\epsilon \rightarrow 0} \frac{\csc(\pi\epsilon) (\Gamma(\epsilon) - 2\Gamma(1-\epsilon)\Gamma(2\epsilon))}{128\pi^{3+2\epsilon} [(x_2 - x_{\mathcal{O}})^2]^{1+2\epsilon} \Gamma(1-\epsilon)} \\
 &= \frac{1}{2^7 \pi^4} f(\tau_2) \frac{\pi^2}{6}. \tag{4.16}
 \end{aligned}$$

Then we rewrite (4.15) as a sum of two terms

$$\begin{aligned}
 \langle W[\mathcal{C}] \mathcal{O}_2(x_{\mathcal{O}}) \rangle_{\text{int}} &= \\
 &\left. \begin{aligned}
 &- \frac{\lambda^2 \cos^2 \phi}{2^3 \sqrt{2} N} \oint d\tau_1 d\tau_2 f(\tau_1) f(\tau_2) \mathcal{I}_1(x_1 - x_2, x_{\mathcal{O}} - x_2) (x_1 - x_2)^2 \\
 &+ \frac{\lambda^2 \cos^2 \phi}{2 \sqrt{2} N} \oint d\tau_1 d\tau_2 f(\tau_1) \left[\mathcal{I}_1(x_1 - x_{\mathcal{O}}, x_2 - x_{\mathcal{O}}) + \mathcal{I}_2(x_2 - x_{\mathcal{O}}, x_1 - x_{\mathcal{O}}) \right] \\
 &- \frac{\lambda^2 \cos^2 \phi}{2^8 \pi^4 \sqrt{2} N} \oint d\tau_1 d\tau_2 f(\tau_1) f(\tau_2) \left[\text{Li}_2 \left(1 - (1 - \cos \tau_{21}) f(\tau_1) \right) \right]
 \end{aligned} \right\} \mathbf{A} \tag{4.17} \\
 &+ \frac{\lambda^2 \cos^2 \phi}{2^9 \pi^4 \sqrt{2} N} \oint d\tau_1 d\tau_2 d\tau_3 \epsilon(\tau_1, \tau_2, \tau_3) f(\tau_1) f(\tau_3) \cot \left(\frac{\tau_{32}}{2} \right) \log \left(\frac{f(\tau_3)}{f(\tau_2)} \right). \quad \mathbf{B}
 \end{aligned}$$

The integrals A and B are computed in appendix E. In particular B has been evaluated analytically obtaining $B = -2\mathbf{L}$, where \mathbf{L} is given in (4.8). The term A has been calculated numerically for different values of the angle ϕ . In figure 5 we plot the ratio $\frac{\mathbf{L}}{\mathbf{A}}$ and from this analysis we conclude that $\mathbf{A} = \mathbf{L}$.⁵

The contribution of the interacting diagrams is therefore

$$\langle W[\mathcal{C}] \mathcal{O}_2(x_{\mathcal{O}}) \rangle_{\text{int}} = -\mathbf{L}. \tag{4.18}$$

⁵For $\phi < \frac{\pi}{32}$ the value of A is much less than its error, while \mathbf{L} is an analytic quantity. Thus in figure 5 we drop the points in that range.

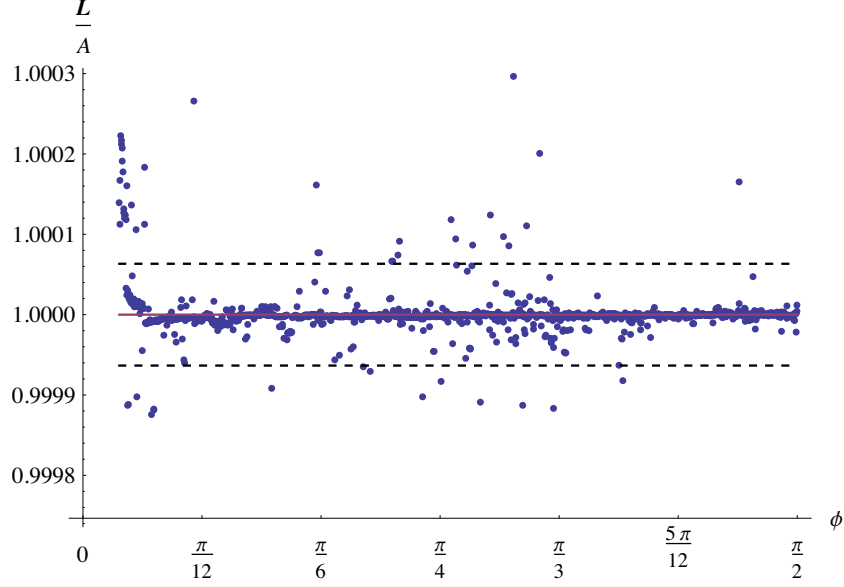


Figure 5. Numerical evaluation of the ratio $\frac{L}{A}$ as a function of ϕ obtained with Wolfram Mathematica routine NIntegrate. The red line is the linear fit of the data and the dashed lines are the upper and lower limit of the Confidence Interval.

Finally, summing up the interacting and the ladder contributions, we obtain

$$\langle W[\mathcal{C}]\mathcal{O}_2(x_{\mathcal{O}}) \rangle = \langle W[\mathcal{C}]\mathcal{O}_2(x_{\mathcal{O}}) \rangle_{\text{int}} + \langle W[\mathcal{C}]\mathcal{O}_2(x_{\mathcal{O}}) \rangle_{\text{ladder}} = \frac{\lambda^2}{192\sqrt{2}N} \quad (4.19)$$

that perfectly fits into the localization result.

A The integrals $\mathcal{I}_1(x, y)$ and $\mathcal{I}_2(x, y)$

The integral $\mathcal{I}_1(x, y)$, defined in (3.10), has been evaluated [21] in momentum space representation and using dimensional regularization ($\omega = 2 + \epsilon$)

$$\begin{aligned} \mathcal{I}_1(x, y) &\equiv \int \frac{d^{2\omega}p_1 d^{2\omega}p_2}{(2\pi)^{4\omega}} \frac{e^{ip_1x + ip_2y}}{p_1^2 p_2^2 (p_1 + p_2)^2} \\ &= \frac{\Gamma(2\omega - 3)}{64\pi^{2\omega}(\omega - 1)} \int_0^1 d\alpha \frac{[\alpha(1 - \alpha)]^{\omega-2}}{[\alpha(x - y)^2 + (1 - \alpha)y^2]^{2\omega-3}} \\ &\quad \times {}_2F_1\left(1, 2\omega - 3, \omega, \frac{(y - \alpha x)^2}{\alpha(x - y)^2 + (1 - \alpha)y^2}\right). \end{aligned} \quad (A.1)$$

From this representation, one obtains the behavior of \mathcal{I}_1 near $x = 0$

$$\mathcal{I}_1(0, y) = \frac{\Gamma^2(\omega - 1)}{64\pi^{2\omega}(\omega - 3)(2 - \omega)} \frac{1}{[y^2]^{2\omega-3}}. \quad (A.2)$$

Since (A.1) is manifestly symmetric under the exchange $x \leftrightarrow y$ and $x \leftrightarrow y - x$, the behavior at $y = 0$ and $y = x$ is similar. The integral $\mathcal{I}_2(x, y)$ is defined as follows [21]

$$\begin{aligned} \mathcal{I}_2(x, y) = & -\frac{\Gamma(2\omega - 3)}{64\pi^{2\omega}(\omega - 1)} \int_0^1 d\alpha \frac{\alpha^{\omega-1}(1-\alpha)^{\omega-2}}{[\alpha(1-\alpha)x^2 + (y-\alpha x)^2]^{2\omega-3}} \\ & \times {}_2F_1\left(1, 2\omega - 3, \omega, \frac{(y-\alpha x)^2}{(y-\alpha x)^2 + \alpha(1-\alpha)x^2}\right). \end{aligned} \quad (\text{A.3})$$

Here we quote its behavior at $x = 0$, $y = 0$ and $y = x$.

At $x = 0$:

$$\mathcal{I}_2(0, y) = -\frac{\Gamma^2(\omega - 1)}{128\pi^{2\omega}(2 - \omega)(2\omega - 3) [(y)^2]^{2\omega-3}}. \quad (\text{A.4})$$

At $y = 0$:

$$\mathcal{I}_2(x, 0) = -\frac{\Gamma(2\omega - 3)\Gamma(3 - \omega)\Gamma(\omega - 1)}{64\pi^{2\omega} [x]^{2\omega-3}} \frac{(\Gamma(\omega - 2) - 2\Gamma(3 - \omega)\Gamma(2\omega - 4))}{4(\omega - 2)^3\Gamma(2 - \omega)\Gamma(2\omega - 4)}. \quad (\text{A.5})$$

At $y = x$:

$$\mathcal{I}_2(x, x) = -\frac{\Gamma(2\omega - 3)\Gamma(2 - \omega)\Gamma(\omega)}{64\pi^{2\omega}(\omega - 1)[x^2]^{2\omega-3}} \frac{1 - \frac{\Gamma(\omega-1)}{\Gamma(3-\omega)\Gamma(2\omega-2)}}{2(\omega - 2)}. \quad (\text{A.6})$$

In section 3 we introduced the following combination of the derivatives of \mathcal{I}_1 and \mathcal{I}_2 :

$$V^\mu(x, y) \equiv \frac{\partial \mathcal{I}_1(x, y)}{\partial x_\mu} - \frac{\partial \mathcal{I}_2(x, y)}{\partial y_\mu}. \quad (\text{A.7})$$

Taking the derivative of (A.1) and (A.3), V^μ can be expressed as [21]

$$V^\mu(x, y) = -\frac{\Gamma(2\omega - 2)x^\mu}{32\pi^{2\omega}(\omega - 1)(x^2)^{2\omega-2}} \int_0^1 d\alpha [\alpha(1-\alpha)]^{1-\omega} {}_2F_1(1, 2\omega - 2; \omega; \xi)(1-\xi)^{2\omega-2}, \quad (\text{A.8})$$

where

$$\xi = \frac{(y - \alpha x)^2}{(y - \alpha x)^2 + \alpha(1 - \alpha)x^2}. \quad (\text{A.9})$$

In particular, setting $\omega = 2$ one has

$$\begin{aligned} V^\mu(x, y) = & -\frac{x^\mu}{32\pi^4 x^2} \int_0^1 d\alpha \frac{1}{\alpha(1-\alpha)x^2 + (y-\alpha x)^2} \\ = & \frac{x^\mu}{32\pi^4 x^2} \frac{\log\left[\frac{y^2}{(x-y)^2}\right]}{(x-y)^2 - y^2} \end{aligned} \quad (\text{A.10})$$

For our purposes, however, it is more useful to rewrite V^μ as

$$\begin{aligned} V^\mu(x, y) = & \frac{1}{32\pi^4 x^2} \left\{ \frac{\partial}{\partial y_\mu} \left[\text{Li}_2\left(1 - \frac{(x-y)^2}{y^2}\right) + \frac{1}{2} \log^2\left(\frac{(x-y)^2}{y^2}\right) \right] \right. \\ & \left. - \frac{1}{2} \log^2\left(\frac{(x-y)^2}{x^2}\right) \right] - \frac{2(x-y)^\mu}{(x-y)^2} \log\left(\frac{y^2}{x^2}\right) \right\}. \end{aligned} \quad (\text{A.11})$$

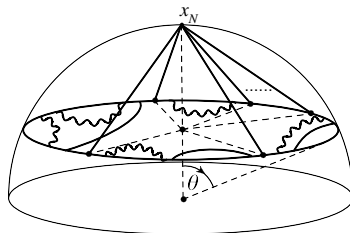


Figure 6. A typical ladder diagram for latitude-north pole correlation function.

B The latitude-north pole correlator

In this appendix we compute the ladder contribution to the correlation function of a Wilson loop lying on a latitude of S^2 and the chiral primary operator \mathcal{O}_J inserted at the north pole to any order in λ (see figure 6). As the generalized connection does not depend on the scalar field Φ^4 (see (3.2)), the operator \mathcal{O}_J effectively reduces to

$$\mathcal{O}_J(x_N) = \left(\frac{2\pi}{\sqrt{\lambda}} \right)^J \frac{1}{\sqrt{J}} \text{Tr}(\Phi_N^3)^J, \quad (\text{B.1})$$

where we use the notation $\Phi_N^3 = \Phi^3(x_N)$.

We have

$$\langle W[\mathcal{C}] \mathcal{O}_J(x_N) \rangle_{\text{ladder}} = \frac{1}{N} \sum_{n=0}^{\infty} \int_0^{2\pi} d\tau_1 \dots \int_0^{\tau_{2n+J-1}} d\tau_{2n+J} \langle \text{Tr}(\mathcal{A}_1 \dots \mathcal{A}_{2n+J}) \mathcal{O}_J(x_N) \rangle, \quad (\text{B.2})$$

where n counts the number of ladder insertions in the Wilson loop. Using the effective propagators (3.3) we get

$$\langle \text{Tr}(\mathcal{A}_1 \dots \mathcal{A}_{2n+J}) \text{Tr}(\Phi_N^3)^J \rangle = \left(\frac{\lambda'}{16\pi^2} \right)^{n+J} \left(\frac{1}{1 - \cos \theta} \right)^J N_{\text{tot}}, \quad (\text{B.3})$$

where N_{tot} is the total number of planar graphs. Any such diagram originates from Wick contractions of this kind

$$\underbrace{\mathcal{A}_1 \mathcal{A}_2 \dots \mathcal{A}_{2s_1+1}}_{2s_1} \underbrace{\mathcal{A}_{2s_1+2} \mathcal{A}_{2s_1+3} \dots \mathcal{A}_{2s_1+2s_2+2}}_{2s_2} \dots // \dots \underbrace{\mathcal{A}_{2n+J-2s_{J-1}} \dots \mathcal{A}_{2n+J-1}}_{2s_{J-1}} \underbrace{\mathcal{A}_{2n+J} \Phi_N^3 \Phi_N^3 \dots // \dots \Phi_N^3}_J \quad (\text{B.4})$$

where $\sum_{i=1}^{J-1} s_i = n$ and the $2s$ generalized connections \mathcal{A}_i under the brackets have to be contracted among themselves. According to [7] the number of these planar contractions is

$$N_s = \frac{(2s)!}{(s+1)!s!}. \quad (\text{B.5})$$

Therefore the total number of planar graphs is

$$N_{\text{tot}} = (2n+J) \sum_{s_1=0}^n N_{s_1} \sum_{s_2=0}^{n-s_1} N_{s_2} \sum_{s_3=0}^{n-s_1-s_2} \dots // \dots \sum_{s_{J-1}=0}^{n-\sum_{i=1}^{J-2} s_i} N_{s_{J-1}} N_{n-\sum_{i=1}^{J-2} s_i-s_{J-1}}, \quad (\text{B.6})$$

where the factor $(2n + J)$ comes from the cyclicity of the trace. Using the recurrence relation [7]

$$N_{n+1} = \sum_{k=0}^n N_{n-k} N_k, \quad (\text{B.7})$$

with $N_0 = 1$, we can perform the sum over s_{J-1} , obtaining

$$(2n + J) \sum_{s_1=0}^n \frac{2s_1!}{s_1!(s_1+1)!} \sum_{s_2=0}^{n-s_1} \frac{2s_2!}{s_2!(s_2+1)!} \sum_{s_3=0}^{n-s_1-s_2} \dots // \dots$$

$$\times \left[\sum_{s_{J-2}=0}^{n-\sum_{i=1}^{J-3} s_i+1} N_{s_{J-2}} N_{n-\sum_{i=1}^{J-3} s_i+1-s_{J-2}} - \frac{(2n - 2\sum_{i=1}^{J-3} s_i + 2)!}{(n - \sum_{i=1}^{J-3} s_i + 1)!(n - \sum_{i=1}^{J-3} s_i + 2)!} \right]. \quad (\text{B.8})$$

Iterating this process $(J - 3)$ -times, we get

$$N_{\text{tot}} = \frac{J(2n + J)!}{n!(n + J)!}. \quad (\text{B.9})$$

Substituting this result into the (B.3) and performing the trivial integrations, we can write

$$\langle W[\mathcal{C}] \mathcal{O}_J(x_N) \rangle_{\text{ladder}} = \frac{1}{N} \frac{\sqrt{J}}{2^J} \left(\frac{A_2}{A_1} \right)^{J/2} \sum_{n=0}^{\infty} \frac{1}{n!(n + J)!} \left(\frac{\sqrt{\lambda'}}{2} \right)^{2n+J}$$

$$= \frac{1}{N} \frac{\sqrt{J}}{2^J} \left(\frac{A_2}{A_1} \right)^{J/2} I_J(\sqrt{\lambda'}). \quad (\text{B.10})$$

Thus the sum of all ladder contribution reproduces the localization result (2.8).

C Summing up interactions I: the details

The evaluation of P_1 . Using the integral representation of \mathcal{I}_1 given in (A.1), we get

$$P_1 = \oint d\tau_1 d\tau_2 \mathcal{I}_1(x_1 - x_2, x_N - x_2) (x_1 - x_2)^2$$

$$= \frac{\Gamma(2\omega - 3)}{2^5 \pi^{2\omega} (\omega - 1)} \frac{\sin^2 \theta}{(1 - \cos \theta)^{2\omega-3}} \oint d\tau_1 d\tau_2 \int_0^1 d\alpha \frac{[\alpha(1 - \alpha)]^{\omega-2} (1 - \cos \tau_{12})}{2^{2\omega-3}}$$

$$\times {}_2F_1 \left(1, 2\omega - 3; \omega; 1 - \alpha(1 - \alpha) \frac{\sin^2 \theta}{(1 - \cos \theta)} (1 - \cos \tau_{12}) \right). \quad (\text{C.1})$$

With the help of the following identity

$${}_2F_1(\alpha, \beta; \gamma; z) = \frac{\Gamma(\gamma)\Gamma(\gamma - \alpha - \beta)}{\Gamma(\gamma - \alpha)\Gamma(\gamma - \beta)} {}_2F_1(\alpha, \beta; \alpha + \beta - \gamma + 1; 1 - z)$$

$$+ (1 - z)^{\gamma - \alpha - \beta} \frac{\Gamma(\gamma)\Gamma(\alpha + \beta - \gamma)}{\Gamma(\alpha)\Gamma(\beta)} {}_2F_1(\gamma - \alpha, \gamma - \beta; \gamma - \alpha - \beta + 1; 1 - z), \quad (\text{C.2})$$

and the series representation of the hypergeometric function, P_1 becomes

$$\begin{aligned} & \frac{1}{2^{6+2\epsilon}\pi^{4+2\epsilon}} \sum_{k=0}^{\infty} \oint d\tau_1 d\tau_2 \int_0^1 d\alpha \left[\frac{(\sin^2 \theta)^{1-\epsilon+k}}{(1-\cos \theta)^{1+\epsilon+k}} \Gamma(\epsilon) \frac{\Gamma(1+\epsilon+k)}{\Gamma(k+1)} [\alpha(1-\alpha)]^k (1-\cos \tau_{12})^{1-\epsilon+k} \right. \\ & \left. + \frac{(\sin^2 \theta)^{1+k}}{(1-\cos \theta)^{1+2\epsilon+k}} \frac{\Gamma(-\epsilon)}{\Gamma(1-\epsilon)} \frac{\Gamma(1+2\epsilon+k)\Gamma(1+\epsilon)}{\Gamma(1+\epsilon+k)} [\alpha(1-\alpha)]^{\epsilon+k} (1-\cos \tau_{12})^{k+1} \right]. \quad (\text{C.3}) \end{aligned}$$

The integrations can now be performed easily, and we obtain

$$\begin{aligned} & \frac{\sqrt{\pi}}{2^{6+2\epsilon}\pi^{3+2\epsilon}} \sum_{k=0}^{\infty} \left[2^{3+k} \frac{(\sin^2 \theta)^{1+k}}{(1-\cos \theta)^{1+2\epsilon+k}} \frac{\Gamma(-\epsilon)}{\Gamma(1-\epsilon)} \frac{\Gamma(1+2\epsilon+k)\Gamma(1+\epsilon)\Gamma(1+\epsilon+k)\Gamma(3/2+k)}{\Gamma(2+2\epsilon+2k)\Gamma(k+2)} \right. \\ & \left. + 2^{3-\epsilon+k} \frac{(\sin^2 \theta)^{1-\epsilon+k}}{(1-\cos \theta)^{1+\epsilon+k}} \Gamma(\epsilon) \frac{\Gamma(1+\epsilon+k)\Gamma(k+1)\Gamma(3/2-\epsilon+k)}{\Gamma(2k+2)\Gamma(2-\epsilon+k)} \right]. \quad (\text{C.4}) \end{aligned}$$

Taking the limit $\epsilon \rightarrow 0$ we see that divergences cancel, and the sum over k gives

$$P_1 = \frac{1}{8\pi^2} \left[\frac{\pi^2}{6} - \text{Li}_2 \left(\sin^2 \frac{\theta}{2} \right) \right]. \quad (\text{C.5})$$

The evaluation of P_2 . Using the integral representation of \mathcal{I}_1 and \mathcal{I}_2 given in (A.1) and (A.3), we get

$$\begin{aligned} P_2 &= \oint d\tau_1 d\tau_2 \left[\mathcal{I}_1(x_1 - x_N, x_2 - x_N) + \mathcal{I}_2(x_2 - x_N, x_1 - x_N) \right] \\ &= \frac{1}{2^{2\omega+3}} \frac{\Gamma(2\omega-3)}{\pi^{2\omega}(\omega-1)} \frac{1}{(1-\cos \theta)^{2\omega-3}} \oint d\tau_1 d\tau_2 \int_0^1 d\alpha \frac{(1-\alpha)[\alpha(1-\alpha)]^{\omega-2}}{[1+\alpha \cos \theta - \alpha(1+\cos \theta) \cos \tau_{21}]^{2\omega-3}} \\ & \quad \times {}_2F_1 \left(1, 2\omega-3, \omega, 1 - \frac{\alpha(1-\alpha)}{1+\alpha \cos \theta - \alpha(1+\cos \theta) \cos \tau_{21}} \right). \quad (\text{C.6}) \end{aligned}$$

With the help of the identity

$${}_2F_1(\alpha, \beta; \gamma; z) = (1-z)^{-\beta} {}_2F_1 \left(\beta, \gamma - \alpha; \gamma; \frac{z}{z-1} \right), \quad (\text{C.7})$$

we arrive to the following expression

$$\begin{aligned} P_2 &= \frac{1}{2^{2\omega+3}} \frac{\Gamma(2\omega-3)}{\pi^{2\omega}(\omega-1)} \frac{1}{(1-\cos \theta)^{2\omega-3}} \oint d\tau_1 d\tau_2 \int_0^1 d\alpha \alpha^{1-\omega} (1-\alpha)^{2-\omega} \\ & \quad \times {}_2F_1 \left(2\omega-3, \omega-1, \omega, -\frac{1-\alpha}{\alpha} - \frac{(1+\cos \theta)(1-\cos \tau_{21})}{1-\alpha} \right). \quad (\text{C.8}) \end{aligned}$$

Exploiting the Mellin-Barnes representation of the hypergeometric function, we recast P_2 as

$$\begin{aligned} & \frac{1}{2^{2\omega+4}} \frac{1}{\pi^{2\omega+1}} \frac{1}{i(1-\cos \theta)^{2\omega-3}} \oint d\tau_1 d\tau_2 \int_0^1 d\alpha \alpha^{1-\omega} (1-\alpha)^{2-\omega} \\ & \quad \times \int_{-i\infty}^{i\infty} dt \frac{\Gamma(2\omega-3+t)\Gamma(\omega-1+t)\Gamma(-t)}{\Gamma(\omega+t)} \left(\frac{1-\alpha}{\alpha} + \frac{(1+\cos \theta)(1-\cos \tau_{21})}{1-\alpha} \right)^t. \quad (\text{C.9}) \end{aligned}$$

We perform a Mellin-Barnes transform also of last factor in (C.9), obtaining

$$-\frac{1}{2^{2\omega+5}} \frac{1}{\pi^{2\omega+2}} \frac{1}{(1-\cos\theta)^{2\omega-3}} \int_{-i\infty}^{i\infty} dt \int_{-i\infty}^{i\infty} ds \frac{\Gamma(2\omega-3+t)\Gamma(s)\Gamma(-t-s)}{(\omega-1+t)} (1+\cos\theta)^{-s} \\ \times \oint d\tau_1 d\tau_2 (1-\cos\tau_{21})^{-s} \int_0^1 d\alpha \alpha^{1-\omega-t-s} (1-\alpha)^{2-\omega+t+2s}. \quad (\text{C.10})$$

Evaluating the integrals over τ_1 , τ_2 and α and setting $\omega = 2 + \epsilon$, we get

$$-\frac{1}{2^{7+2\epsilon}} \frac{\sqrt{\pi}}{\pi^{5+2\epsilon}} \int_{-i\infty}^{i\infty} dt \int_{-i\infty}^{i\infty} ds \frac{(1+\cos\theta)^{-s}}{(1-\cos\theta)^{1+2\epsilon}} 2^{-s} \frac{\Gamma(1+2\epsilon+t)\Gamma(s)\Gamma(-t-s)\Gamma(\frac{1}{2}-s)}{(1+\epsilon+t)\Gamma(1-s)\Gamma(s-2\epsilon+1)} \\ \times \Gamma(-\epsilon-t-s)\Gamma(1+t+2s-\epsilon). \quad (\text{C.11})$$

Analyzing the singularity structure of the integrand, it is possible to choose a contour of integration for s and t that allows us to take $\epsilon = 0$ and satisfies

$$0 < \text{Re}(s) < 1/2, \quad -1 < \text{Re}(t) < -\text{Re}(s). \quad (\text{C.12})$$

Shifting $t \rightarrow t - s$ and expressing everything in terms of Γ -functions (C.11) becomes

$$-\frac{1}{2^7} \frac{\sqrt{\pi}}{\pi^5} \int_{-i\infty}^{i\infty} ds \frac{(1+\cos\theta)^{-s}}{(1-\cos\theta)} \frac{2^{-s} \sin(\pi s) \Gamma(\frac{1}{2}-s) \Gamma(s)}{\pi s} \\ \times \int_{-i\infty}^{i\infty} dt \left[\Gamma(t-s) \Gamma(-t)^2 \Gamma(s+t+1) - \frac{\Gamma(t-s) \Gamma(-t)^2 \Gamma(s+t+1) \Gamma(t-s+1)}{\Gamma(t-s+2)} \right]. \quad (\text{C.13})$$

The integral over t can be performed using the two Barnes lemmas, obtaining

$$\frac{i}{2^6} \frac{\sqrt{\pi}}{\pi^4} \int_{-i\infty}^{i\infty} ds \frac{(1+\cos\theta)^{-s}}{(1-\cos\theta)} 2^{-s} \Gamma\left(\frac{1}{2}-s\right) \Gamma(s)^2 \Gamma(-s) \left(1 - \frac{\Gamma(1-s)^2}{\Gamma(1-2s)}\right). \quad (\text{C.14})$$

Finally the integral over s is easily done through residue theorem, and we get

$$P_2 = \frac{1}{96\pi^2} \frac{1}{1-\cos\theta} \left[\pi^2 - 3 \text{Li}_2\left(\sin^2 \frac{\theta}{2}\right) - 6 \left(\log^2\left(\cos \frac{\theta}{2}\right) + \arctan^2\left(\sqrt{1+2\cos\theta}\right) \right) \right]. \quad (\text{C.15})$$

The evaluation of P_3 . The evaluation of P_3 is straightforward: taking $\omega = 2 + \epsilon$ we get

$$P_3 = \oint d\tau_1 d\tau_2 \left[\mathcal{I}_2(x_2 - x_N, x_2 - x_N) + \mathcal{I}_1(0, x_2 - x_N) \right] \\ = - \frac{\csc(\pi\epsilon) (\Gamma(\epsilon) - 2\Gamma(1-\epsilon)\Gamma(2\epsilon))}{2^{6+2\epsilon} \pi^{1+2\epsilon} (1-\cos\theta)^{1+2\epsilon} \Gamma(1-\epsilon)} \\ = \frac{1}{192} \frac{1}{1-\cos\theta} \quad \epsilon \rightarrow 0. \quad (\text{C.16})$$

The evaluation of P_4 . We have

$$P_4 = \oint d\tau_1 d\tau_3 \text{Li}_2 \left(1 - \frac{\sin^2 \theta}{1-\cos\theta} (1-\cos\tau_{31}) \right) \\ = 8\pi \int_0^{\pi/2} d\tau \text{Li}_2 (1 - K(\theta) \sin^2 \tau), \quad (\text{C.17})$$

where $K(\theta) = 4 \cos^2 \frac{\theta}{2}$. Using the integral representation of the dilogarithm and changing variable to $x = \sin \tau$, we obtain

$$\begin{aligned} P_4 &= -8\pi \int_0^1 ds \int_0^1 dx \frac{\log[1 - s(1 - K(\theta)x^2)]}{s\sqrt{1-x^2}} \\ &= \frac{2}{3}\pi^4 - 8\pi^2 \int_0^1 \frac{ds}{s} \log \left[\frac{1}{2} \left(1 + \sqrt{1 + \frac{K(\theta)s}{1-s}} \right) \right] \\ &= \frac{\pi^4}{6} - 2\pi^2 \log^2(2) - 8\pi^2 \int_2^K dK' \frac{d}{dK'} \int_0^1 \frac{ds}{s} \log \left[\frac{1}{2} \left(1 + \sqrt{1 + \frac{K'[\theta]s}{1-s}} \right) \right]. \end{aligned} \quad (\text{C.18})$$

Taking the derivative and interchanging the order of integration we get

$$P_4 = \frac{2}{3}\pi^4 - 8\pi^2 \left[\log^2 \left(\cos \frac{\theta}{2} \right) + \arctan^2 \left(\sqrt{1 + 2 \cos \theta} \right) \right]. \quad (\text{C.19})$$

D Some useful integrals

In this appendix we give the integrals \mathcal{J}_n and $\tilde{\mathcal{J}}$ needed to evaluate (4.6):

$$\mathcal{J}_n = \int_0^{2\pi} d\tau \tau^n f(\tau), \quad \tilde{\mathcal{J}} = \int_0^{2\pi} d\tau_1 \tau_1 f(\tau_1) \int_{\tau_1}^{2\pi} d\tau_2 f(\tau_2), \quad (\text{D.1})$$

with $f(\tau)$ given in (4.3) (henceforth we set $\sin \phi = b$, thus $\sigma = \sqrt{\frac{1+b}{1-b}}$).

The integral \mathcal{J}_0 and \mathcal{J}_1 are straightforward. Making the change of variables $\tan \frac{\tau}{2} = x$, \mathcal{J}_0 becomes

$$\mathcal{J}_0 = \frac{2}{1-b} \int_0^\infty \frac{dx}{1 + \sigma^2 x^2} + (b \rightarrow -b) = \frac{2\pi}{\sqrt{1-b^2}}. \quad (\text{D.2})$$

For \mathcal{J}_1 , periodicity of $f(\tau)$ allows us to write

$$\mathcal{J}_1 = \pi \int_{-\pi}^\pi d\tau \frac{1}{1 + b \cos \tau} = \pi \mathcal{J}_0. \quad (\text{D.3})$$

The evaluation of \mathcal{J}_2 is a bit tricky. Again using periodicity and the change of variables $\tan \frac{\tau}{2} = x$, we can write

$$\mathcal{J}_2 = \pi^2 \mathcal{J}_0 + \frac{16}{\sqrt{1-b^2}} \mathcal{F}(\sigma), \quad (\text{D.4})$$

where

$$\mathcal{F}(\sigma) = \int_0^\infty dx \frac{\arctan^2 \sigma x}{1 + x^2}. \quad (\text{D.5})$$

First we evaluate the derivative of $\mathcal{F}(\sigma)$

$$\mathcal{F}'(\sigma) = \frac{1}{\sigma^2} \int_{-\infty}^\infty dx \frac{x \arctan \sigma x}{(1+x^2)(1/\sigma^2+x^2)} = \frac{\pi}{\sigma^2-1} \log \left(\frac{1+\sigma}{2} \right), \quad (\text{D.6})$$

and then we write

$$\begin{aligned} \mathcal{F}(\sigma) &= \mathcal{F}(1) + \int_1^\sigma d\sigma' \mathcal{F}'(\sigma') \\ &= \frac{1}{3} \left(\frac{\pi}{2} \right)^3 - \frac{\pi}{2} \left[\frac{1}{2} \log^2 \left(\frac{1+\sigma}{2} \right) + \text{Li}_2 \left(\frac{1-\sigma}{2} \right) \right]. \end{aligned} \quad (\text{D.7})$$

Finally, substituting this result in (D.4), we obtain:

$$\mathcal{J}_2 = \frac{4\pi}{\sqrt{1-b^2}} \left[\frac{2}{3}\pi^2 - 2\text{Li}_2\left(\frac{1-\sigma}{2}\right) - \log^2\left(\frac{1+\sigma}{2}\right) \right]. \quad (\text{D.8})$$

The integral $\tilde{\mathcal{J}}$ can be treated in a similar way, with the change of variables $x_{1,2} = \cot\left(\frac{\tau_{1,2}}{2}\right)$, one has

$$\tilde{\mathcal{J}} = \frac{8}{(1+b)^2} \int_{-\infty}^{\infty} dx_1 \frac{\text{arccot}(x_1)}{1 + \frac{x_1^2}{\sigma^2}} \int_{-\infty}^{x_1} dx_2 \frac{1}{1 + \frac{x_2^2}{\sigma^2}}. \quad (\text{D.9})$$

Performing the integration over x_2 and integrating by parts we get:

$$\begin{aligned} \tilde{\mathcal{J}} &= \frac{\pi^3}{1-b^2} + \frac{8}{1-b^2} \int_{-\infty}^{\infty} dx_1 \frac{\arctan(x_1/\sigma)^2}{1+x_1^2} \\ &= \frac{\pi^3}{1-b^2} - \frac{8}{1-b^2} \mathcal{F}\left(\frac{1}{\sigma}\right), \end{aligned} \quad (\text{D.10})$$

where $\mathcal{F}(\sigma)$ is given in (D.7).

E Summing up interactions II: the details

In this appendix we evaluate the contribution to (4.17), called A, i.e.

$$\begin{aligned} A &= -\frac{\lambda^2 \cos^2 \phi}{2^3 \sqrt{2} N} \oint d\tau_1 d\tau_2 f(\tau_1) f(\tau_2) \mathcal{I}_1(x_1 - x_2, x_{\mathcal{O}} - x_2) (x_1 - x_2)^2 \\ &\quad + \frac{\lambda^2 \cos^2 \phi}{2\sqrt{2} N} \oint d\tau_1 d\tau_2 f(\tau_1) \left[\mathcal{I}_1(x_1 - x_{\mathcal{O}}, x_2 - x_{\mathcal{O}}) + \mathcal{I}_2(x_2 - x_{\mathcal{O}}, x_1 - x_{\mathcal{O}}) \right] \\ &\quad - \frac{\lambda^2 \cos^2 \phi}{2^8 \pi^4 \sqrt{2} N} \oint d\tau_1 d\tau_2 f(\tau_1) f(\tau_2) \left[\text{Li}_2\left(1 - (1 - \cos \tau_{21})f(\tau_1)\right) \right], \end{aligned} \quad (\text{E.1})$$

with \mathcal{I}_1 and \mathcal{I}_2 given in (A.1) and (A.3). The new feature of this contribution with respect to the integrals evaluated in appendix C is the appearance of the functions $f(\tau_i)$ (also in the argument of the dilogarithm and the hypergeometric function). Because of this fact, we are not able to compute (E.1) analytically and we have to resort to its numerical evaluation for different values of the angle $\phi \in [0, \pi/2]$, which identifies the position of the operator on the sphere. The results are shown in figure 7.

In particular, the vanishing of A at $\phi = 0$ (i.e. the operator on the north-pole) is consistent with analytic results of section 3.

The last integral in (4.17), i.e. the term B, is

$$B = \frac{\lambda^2 \cos^2 \phi}{2^9 \pi^4 \sqrt{2} N} \oint d\tau_1 d\tau_2 d\tau_3 \epsilon(\tau_1, \tau_2, \tau_3) f(\tau_1) f(\tau_3) F(\tau_3, \tau_2), \quad (\text{E.2})$$

with

$$F(\tau_3, \tau_2) = F(\tau_2, \tau_3) = \cot\left(\frac{\tau_{32}}{2}\right) \log\left(\frac{f(\tau_3)}{f(\tau_2)}\right). \quad (\text{E.3})$$

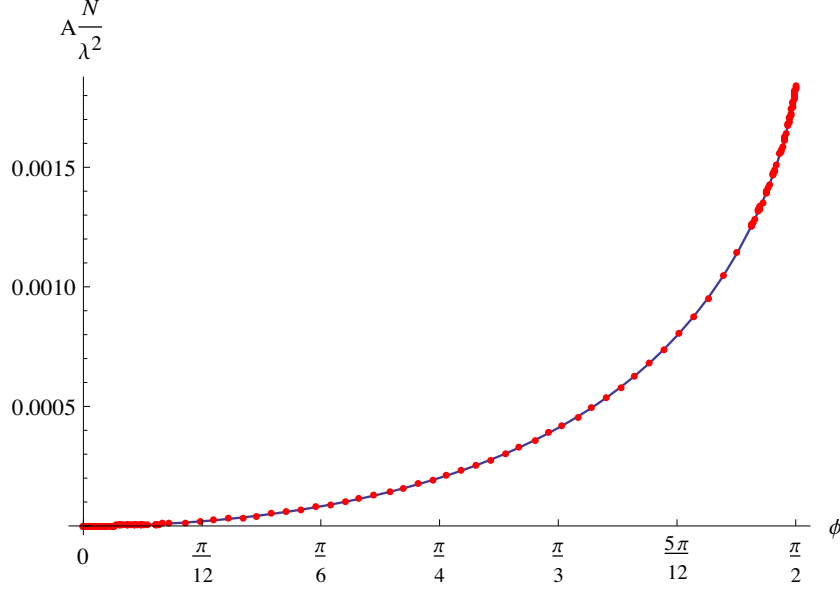


Figure 7. Numerical evaluation of the quantity $A \frac{N}{\lambda^2}$ as a function of the angle ϕ obtained with Wolfram Mathematica routine NIntegrate.

It is useful to express $f(\tau)$ in terms of its primitive $g(\tau)$

$$g(\tau) = \frac{2}{\sqrt{1-b^2}} \operatorname{arccot} \left(\frac{1}{\sigma} \cot \frac{\tau_i}{2} \right), \quad (\text{E.4})$$

with

$$g(0) = \lim_{\tau \rightarrow 0^+} g(\tau) = 0, \quad g(2\pi) = \lim_{\tau \rightarrow 2\pi^-} g(\tau) = \frac{2\pi}{\sqrt{1-b^2}}. \quad (\text{E.5})$$

Then using the integration by parts and (3.17) and (3.15), we can evaluate one of the three integrals, obtaining

$$\begin{aligned} B = & \frac{\lambda^2 \cos^2 \phi}{2^8 \pi^4 \sqrt{2} N} \oint d\tau_2 \left\{ \oint d\tau_3 (g(\tau_3) - g(\tau_2)) f(\tau_3) F(\tau_3, \tau_2) \right. \\ & \left. + \frac{1}{2} g(2\pi) \left[\int_0^{\tau_2} d\tau_3 f(\tau_3) F(\tau_3, \tau_2) - \int_{\tau_2}^{2\pi} d\tau_3 f(\tau_3) F(\tau_3, \tau_2) \right] \right\}. \end{aligned} \quad (\text{E.6})$$

With the usual change of variables $x = \cot \frac{\tau}{2}$, in both integrals, we can evaluate one of the two integrals, obtaining

$$B = \frac{\lambda^2}{2^4 \pi^2 \sqrt{2} N} \left\{ \log^2 \left(\frac{2\sigma}{\sigma+1} \right) - \frac{1}{2\pi} \int_0^\infty dy \frac{\sigma \log^2 \left(\frac{1+y^2}{\sigma^2+y^2} \right)}{\sigma^2+y^2} \right\}. \quad (\text{E.7})$$

The integral in (E.7) is done by expanding the integrand in power series in σ at $\sigma = 1$

$$\begin{aligned} \int_0^\infty dy \frac{\sigma \log^2 \left(\frac{1+y^2}{\sigma^2+y^2} \right)}{\sigma^2+y^2} = & \int_{-\infty}^\infty dy \sum_{n=2}^\infty \sum_{j=1}^{n-1} \frac{i^{n+1}}{2(n-j)(y^2+1)^{n+1}} ((i-y)^{n-j} + (i+y)^{n-j}) \\ & \times (i-y)^{j+1} \left(H_j - \beta_{\frac{i+y}{i-y}}(1+j, 0) - \log \left(\frac{2y}{y-i} \right) \right) (\sigma-1)^n, \end{aligned} \quad (\text{E.8})$$

where $H_n = \sum_{k=1}^n \frac{1}{k}$ are the harmonic numbers and $\beta_z(a, b) = z^a \sum_{n=0}^{\infty} \frac{(1-b)_n}{n!(a+n)} z^n$ is the incomplete β -function.

Given the following series expansion

$$\left(H_j - \beta_{\frac{i+y}{i-y}}(1+j, 0) - \log\left(\frac{2y}{y-i}\right) \right) = \sum_{k=1}^j \frac{1}{k} \left(\frac{(i+y)^k}{(i-y)^k} + 1 \right), \quad (\text{E.9})$$

Eq. (E.8) becomes

$$\begin{aligned} & \sum_{n=2}^{\infty} \sum_{j=1}^{n-1} \sum_{k=1}^j \int_{-\infty}^{\infty} dy \frac{i^{n+1}}{2(n-j)(y^2+1)^{n+1}} ((i-y)^{n-j} + (i+y)^{n-j}) \frac{1}{k} \left(\frac{(i+y)^k}{(i-y)^k} + 1 \right) (\sigma-1)^n \\ &= \sum_{n=2}^{\infty} \sum_{j=1}^{n-1} \sum_{k=1}^j \frac{(\sigma-1)^n}{\pi^2 k \Gamma(k+1)(n-j)\Gamma(k+n-j)} \left[i e^{-i\pi k} 2^{-n-2} \sin(\pi j) \sin(\pi(k-j)) \right. \\ & \quad \times \left(\pi^2(-k) \csc(\pi j) \csc(\pi(k-j)) \Gamma(k+n-j) \left(\pi e^{i\pi k} (-2)^n \csc(\pi k) {}_2\tilde{F}_1\left(1, 1-n; 2-k; \frac{1}{2}\right) \right. \right. \\ & \quad \left. \left. + 2(-1 + e^{2i\pi k}) \Gamma(n) \Gamma(k-n) \right) - \pi e^{i\pi k} \Gamma(k+1) \sin(\pi j) (\pi \csc^2(\pi j) \csc(\pi(k-j))) \right. \\ & \quad \times \left(\pi 2^n \csc(\pi(k-j)) {}_2\tilde{F}_1\left(1, 1-n; -k-n+j+2; \frac{1}{2}\right) + 2(-1)^n \Gamma(k+n-j) \right. \\ & \quad \times \left(\beta_{\frac{1}{2}}(k-j, -k-n+j+1) + \beta_{\frac{1}{2}}(k-n, 1-k) + \beta_{\frac{1}{2}}(-j, -n+j+1) + \beta_{\frac{1}{2}}(-n+j+1, -j) \right) \Big) \\ & \quad \left. + 4i\Gamma(n) (\pi(-1)^n \csc^2(\pi j) \Gamma(k-j) + \Gamma(-j) \csc(\pi(k-j)) \Gamma(-n+j+1) \Gamma(k+n-j)) \right) \Big] \\ &= \sum_{n=2}^{\infty} \frac{2^{-n} \pi e^{i\pi n}}{n^2} \left[2^n n \left({}_3F_2\left(1, 1, 1-n; 2, 2; \frac{1}{2}\right) + 2(\Phi(2, 1, n) + \psi^{(0)}(n) + \gamma) - \log(4) \right) \right. \\ & \quad \left. + 2n\Phi\left(\frac{1}{2}, 1, n\right) + 2i\pi n - 2 \right] (\sigma-1)^n \\ &= -\pi \left[2\text{Li}_2\left(\frac{1-\sigma}{2}\right) + 2\text{Li}_2\left(\frac{\sigma-1}{2\sigma}\right) - \log(\sigma)(\log(\sigma) - 2\log(\sigma+1) + \log(4)) \right], \quad (\text{E.10}) \end{aligned}$$

where γ is the Euler-Mascheroni constant, ${}_2\tilde{F}_1(a, b, c, z) = \frac{{}_2F_1(a, b, c, z)}{\Gamma(c)}$ is the regularized hypergeometric function, $\Phi(z, a, s) = \sum_{n=0}^{\infty} \frac{z^n}{(a+n)^s}$ is the Lerch transcendent function and $\psi^{(0)}(z) = \frac{d}{dz} \log \Gamma(z)$ is the digamma function.

Finally, including the result (E.10) in (E.7), we obtain

$$\begin{aligned} B &= \frac{\lambda^2}{2^4 \pi^2 \sqrt{2} N} \left\{ \log^2\left(\frac{2\sigma}{\sigma+1}\right) + \text{Li}_2\left(\frac{1-\sigma}{2}\right) + \text{Li}_2\left(\frac{\sigma-1}{2\sigma}\right) - \frac{1}{2} \log(\sigma) \log\left(\frac{4\sigma}{(\sigma+1)^2}\right) \right\} \\ &= \frac{\lambda^2}{2^5 \pi^2 \sqrt{2} N} \left[\log^2\left(\frac{2\sigma}{1+\sigma}\right) + \log^2\left(\frac{1+\sigma}{2}\right) + 2\text{Li}_2\left(\frac{1-\sigma}{2}\right) + 2\text{Li}_2\left(\frac{\sigma-1}{2\sigma}\right) \right] \\ &= -2\mathbf{L}. \quad (\text{E.11}) \end{aligned}$$

where \mathbf{L} is defined in (4.8).

Open Access. This article is distributed under the terms of the Creative Commons Attribution License ([CC-BY 4.0](https://creativecommons.org/licenses/by/4.0/)), which permits any use, distribution and reproduction in any medium, provided the original author(s) and source are credited.

References

- [1] N.A. Nekrasov, *Seiberg-Witten prepotential from instanton counting*, *Adv. Theor. Math. Phys.* **7** (2004) 831 [[hep-th/0206161](#)] [[INSPIRE](#)].
- [2] N. Nekrasov and A. Okounkov, *Seiberg-Witten theory and random partitions*, [hep-th/0306238](#) [[INSPIRE](#)].
- [3] V. Pestun, *Localization of gauge theory on a four-sphere and supersymmetric Wilson loops*, *Commun. Math. Phys.* **313** (2012) 71 [[arXiv:0712.2824](#)] [[INSPIRE](#)].
- [4] A. Kapustin, B. Willett and I. Yaakov, *Exact results for Wilson loops in superconformal Chern-Simons theories with matter*, *JHEP* **03** (2010) 089 [[arXiv:0909.4559](#)] [[INSPIRE](#)].
- [5] J. Gomis, T. Okuda and V. Pestun, *Exact results for 't Hooft loops in gauge theories on S^4* , *JHEP* **05** (2012) 141 [[arXiv:1105.2568](#)] [[INSPIRE](#)].
- [6] N. Drukker, T. Okuda and F. Passerini, *Exact results for vortex loop operators in 3d supersymmetric theories*, *JHEP* **07** (2014) 137 [[arXiv:1211.3409](#)] [[INSPIRE](#)].
- [7] J.K. Erickson, G.W. Semenoff and K. Zarembo, *Wilson loops in $N = 4$ supersymmetric Yang-Mills theory*, *Nucl. Phys. B* **582** (2000) 155 [[hep-th/0003055](#)] [[INSPIRE](#)].
- [8] N. Drukker and D.J. Gross, *An exact prediction of $\mathcal{N} = 4$ SUSYM theory for string theory*, *J. Math. Phys.* **42** (2001) 2896 [[hep-th/0010274](#)] [[INSPIRE](#)].
- [9] F. Passerini and K. Zarembo, *Wilson loops in $\mathcal{N} = 2$ super-Yang-Mills from matrix model*, *JHEP* **09** (2011) 102 [Erratum *ibid.* **1110** (2011) 065] [[arXiv:1106.5763](#)] [[INSPIRE](#)].
- [10] J.G. Russo and K. Zarembo, *Large- N limit of $N = 2$ $SU(N)$ gauge theories from localization*, *JHEP* **10** (2012) 082 [[arXiv:1207.3806](#)] [[INSPIRE](#)].
- [11] F. Bigazzi, A.L. Cotrone, L. Griguolo and D. Seminara, *A novel cross-check of localization and non conformal holography*, *JHEP* **03** (2014) 072 [[arXiv:1312.4561](#)] [[INSPIRE](#)].
- [12] N. Drukker, S. Giombi, R. Ricci and D. Trancanelli, *Supersymmetric Wilson loops on S^3* , *JHEP* **05** (2008) 017 [[arXiv:0711.3226](#)] [[INSPIRE](#)].
- [13] A. Dymarsky and V. Pestun, *Supersymmetric Wilson loops in $\mathcal{N} = 4$ SYM and pure spinors*, *JHEP* **04** (2010) 115 [[arXiv:0911.1841](#)] [[INSPIRE](#)].
- [14] V. Cardinali, L. Griguolo and D. Seminara, *Impure Aspects of Supersymmetric Wilson Loops*, *JHEP* **06** (2012) 167 [[arXiv:1202.6393](#)] [[INSPIRE](#)].
- [15] A. Bassetto and L. Griguolo, *Two-dimensional QCD, instanton contributions and the perturbative Wu-Mandelstam-Leibbrandt prescription*, *Phys. Lett. B* **443** (1998) 325 [[hep-th/9806037](#)] [[INSPIRE](#)].
- [16] V. Pestun, *Localization of the four-dimensional $\mathcal{N} = 4$ SYM to a two-sphere and $1/8$ BPS Wilson loops*, *JHEP* **12** (2012) 067 [[arXiv:0906.0638](#)] [[INSPIRE](#)].
- [17] G.W. Moore, N. Nekrasov and S. Shatashvili, *Integrating over Higgs branches*, *Commun. Math. Phys.* **209** (2000) 97 [[hep-th/9712241](#)] [[INSPIRE](#)].
- [18] A.A. Gerasimov and S.L. Shatashvili, *Higgs Bundles, Gauge Theories and Quantum Groups*, *Commun. Math. Phys.* **277** (2008) 323 [[hep-th/0609024](#)] [[INSPIRE](#)].
- [19] A.A. Gerasimov and S.L. Shatashvili, *Two-dimensional gauge theories and quantum integrable systems*, [arXiv:0711.1472](#) [[INSPIRE](#)].

- [20] S. Giombi, V. Pestun and R. Ricci, *Notes on supersymmetric Wilson loops on a two-sphere*, *JHEP* **07** (2010) 088 [[arXiv:0905.0665](#)] [[INSPIRE](#)].
- [21] A. Bassetto, L. Griguolo, F. Pucci and D. Seminara, *Supersymmetric Wilson loops at two loops*, *JHEP* **06** (2008) 083 [[arXiv:0804.3973](#)] [[INSPIRE](#)].
- [22] D. Young, *BPS Wilson Loops on S^2 at Higher Loops*, *JHEP* **05** (2008) 077 [[arXiv:0804.4098](#)] [[INSPIRE](#)].
- [23] A. Bassetto et al., *Correlators of supersymmetric Wilson-loops, protected operators and matrix models in $\mathcal{N} = 4$ SYM*, *JHEP* **08** (2009) 061 [[arXiv:0905.1943](#)] [[INSPIRE](#)].
- [24] A. Bassetto et al., *Correlators of supersymmetric Wilson loops at weak and strong coupling*, *JHEP* **03** (2010) 038 [[arXiv:0912.5440](#)] [[INSPIRE](#)].
- [25] S. Giombi and V. Pestun, *The 1/2 BPS 't Hooft loops in $\mathcal{N} = 4$ SYM as instantons in 2d Yang-Mills*, *J. Phys. A* **46** (2013) 095402 [[arXiv:0909.4272](#)] [[INSPIRE](#)].
- [26] D. Correa, J. Henn, J. Maldacena and A. Sever, *An exact formula for the radiation of a moving quark in $\mathcal{N} = 4$ super Yang-Mills*, *JHEP* **06** (2012) 048 [[arXiv:1202.4455](#)] [[INSPIRE](#)].
- [27] B. Fiol, B. Garolera and A. Lewkowycz, *Exact results for static and radiative fields of a quark in $\mathcal{N} = 4$ super Yang-Mills*, *JHEP* **05** (2012) 093 [[arXiv:1202.5292](#)] [[INSPIRE](#)].
- [28] N. Gromov and A. Sever, *Analytic Solution of Bremsstrahlung TBA*, *JHEP* **11** (2012) 075 [[arXiv:1207.5489](#)] [[INSPIRE](#)].
- [29] N. Gromov, F. Levkovich-Maslyuk and G. Sizov, *Analytic Solution of Bremsstrahlung TBA II: Turning on the Sphere Angle*, *JHEP* **10** (2013) 036 [[arXiv:1305.1944](#)] [[INSPIRE](#)].
- [30] S. Giombi and V. Pestun, *Correlators of local operators and 1/8 BPS Wilson loops on S^2 from 2d YM and matrix models*, *JHEP* **10** (2010) 033 [[arXiv:0906.1572](#)] [[INSPIRE](#)].
- [31] G.W. Semenoff and K. Zarembo, *More exact predictions of SUSYM for string theory*, *Nucl. Phys. B* **616** (2001) 34 [[hep-th/0106015](#)] [[INSPIRE](#)].
- [32] G.W. Semenoff and D. Young, *Exact 1/4 BPS Loop: Chiral primary correlator*, *Phys. Lett. B* **643** (2006) 195 [[hep-th/0609158](#)] [[INSPIRE](#)].
- [33] S. Giombi and V. Pestun, *Correlators of Wilson Loops and Local Operators from Multi-Matrix Models and Strings in AdS*, *JHEP* **01** (2013) 101 [[arXiv:1207.7083](#)] [[INSPIRE](#)].
- [34] K. Zarembo, *Holographic three-point functions of semiclassical states*, *JHEP* **09** (2010) 030 [[arXiv:1008.1059](#)] [[INSPIRE](#)].
- [35] M.S. Costa, R. Monteiro, J.E. Santos and D. Zoakos, *On three-point correlation functions in the gauge/gravity duality*, *JHEP* **11** (2010) 141 [[arXiv:1008.1070](#)] [[INSPIRE](#)].
- [36] J. Escobedo, N. Gromov, A. Sever and P. Vieira, *Tailoring three-point functions and integrability*, *JHEP* **09** (2011) 028 [[arXiv:1012.2475](#)] [[INSPIRE](#)].
- [37] O. Aharony, O. Bergman, D.L. Jafferis and J. Maldacena, *$\mathcal{N} = 6$ superconformal Chern-Simons-matter theories, M2-branes and their gravity duals*, *JHEP* **10** (2008) 091 [[arXiv:0806.1218](#)] [[INSPIRE](#)].
- [38] V. Cardinali, L. Griguolo, G. Martelloni and D. Seminara, *New supersymmetric Wilson loops in ABJ(M) theories*, *Phys. Lett. B* **718** (2012) 615 [[arXiv:1209.4032](#)] [[INSPIRE](#)].

- [39] M.S. Bianchi, L. Griguolo, M. Leoni, S. Penati and D. Seminara, *BPS Wilson loops and Bremsstrahlung function in $ABJ(M)$: a two loop analysis*, *JHEP* **06** (2014) 123 [[arXiv:1402.4128](#)] [[INSPIRE](#)].
- [40] N. Drukker, *1/4 BPS circular loops, unstable world-sheet instantons and the matrix model*, *JHEP* **09** (2006) 004 [[hep-th/0605151](#)] [[INSPIRE](#)].
- [41] N. Drukker and J. Plefka, *Superprotected n -point correlation functions of local operators in $\mathcal{N} = 4$ super Yang-Mills*, *JHEP* **04** (2009) 052 [[arXiv:0901.3653](#)] [[INSPIRE](#)].
- [42] A.A. Migdal, *Gauge Transitions in Gauge and Spin Lattice Systems*, *Sov. Phys. JETP* **42** (1975) 743 [*Zh. Eksp. Teor. Fiz.* **69** (1975) 1457] [[INSPIRE](#)].
- [43] E. Witten, *On quantum gauge theories in two-dimensions*, *Commun. Math. Phys.* **141** (1991) 153 [[INSPIRE](#)].
- [44] N. Beisert, C. Kristjansen, J. Plefka, G.W. Semenoff and M. Staudacher, *BMN correlators and operator mixing in $\mathcal{N} = 4$ super Yang-Mills theory*, *Nucl. Phys. B* **650** (2003) 125 [[hep-th/0208178](#)] [[INSPIRE](#)].